The Journal of Immunology

Identification of Immune Effectors Essential to the Control of Primary and Secondary Intranasal Infection with *Brucella melitensis* in Mice

Delphine Hanot Mambres, Arnaud Machelart, Georges Potemberg, Carl De Trez, Bernhard Ryffel, Jean-Jacques Letesson and Eric Muraille

J Immunol published online 1 April 2016
http://www.jimmunol.org/content/early/2016/04/01/jimmunol.1502265

The Journal of Immunology is published twice each month by The American Association of Immunologists, Inc., 9650 Rockville Pike, Bethesda, MD 20814-3994.

Print ISSN: 0022-1767 Online ISSN: 1550-6606.

Published April 1, 2016, doi:10.4049/jimmunol.1502265

Identification of Immune Effectors Essential to the Control of Primary and Secondary Intranasal Infection with *Brucella melitensis* in Mice

Delphine Hanot Mambres,*,[1] Arnaud Machelart,*,[1] Georges Potemberg,* Carl De Trez,[†] Bernhard Ryffel,[‡,§] Jean-Jacques Letesson,* and Eric Muraille*,[¶]

The mucosal immune system represents the first line of defense against *Brucella* infection in nature. We used genetically deficient mice to identify the lymphocytes and signaling pathways implicated in the control of primary and secondary intranasal infection with *B. melitensis*. Our analysis of primary infection demonstrated that the effectors implicated differ at the early and late stages and are dependent on the organ. TCR-δ, TAP1, and IL-17RA deficiency specifically affects early control of *Brucella* in the lungs, whereas MHC class II (MHCII) and IFN-γR deficiency impairs late control in the lungs, spleen, and liver. Interestingly, IL-12p35$^{-/-}$ mice display enhanced *Brucella* growth in the spleen but not in the lungs or liver. Secondary intranasal infections are efficiently contained in the lung. In contrast to an i.p. infectious model, in which IL-12p35, MHCII, and B cells are strictly required for the control of secondary infection, we observed that only TCR-β deficiency or simultaneous neutralization of IL-12p35– and IL-17A–dependent pathways impairs the memory protective response against a secondary intranasal infection. Protection is not affected by TCR-δ, MHCII, TAP1, B cell, IL-17RA, or IL-12p35 deficiency, suggesting that CD4$^+$ and CD8$^+$ α/β$^+$ T cells are sufficient to mount a protective immune response and that an IL-17A–mediated response can compensate for the partial deficiency of an IFN-γ–mediated response to control a *Brucella* challenge. These findings demonstrate that the nature of the protective memory response depends closely on the route of infection and highlights the role of IFN-γ–and IL-17RA–mediated responses in the control of mucosal infection by *Brucella*. *The Journal of Immunology*, 2016, 196: 000–000.

Brucella (alpha-proteobacteria) are facultative intracellular Gram-negative coccobacilli that infect mammals and cause brucellosis. Human brucellosis is a zoonotic infection transmitted through ingestion, inhalation, or contact of contaminated animal products with the conjunctiva or skin lesions (1). *Brucella* display strong tissue tropism for the reticuloendothelial and reproductive systems, with a stealthy intracellular lifestyle that limits exposure to protective immune responses (reviewed in Ref. 2). The furtive nature of *Brucella* is attributed, in large part, to the weak agonist activity of its LPS and active suppression of the innate immune response by immunoregulatory factors such as TIR-containing proteins that inhibit MyD88 signaling pathways. Although rarely fatal, *Brucella* can cause a devastating multiorgan disease in humans with serious health complications in the absence of prolonged antibiotic treatment (3). Despite significant progress, the incidence of human brucellosis remains very high in endemic areas (4) and is considered to be largely underestimated (5). In addition, *Brucella* species have been weaponized by several governments and are classified as category B threat agents (6). Because complete eradication of *Brucella* is unpractical because of its presence in a wide range of wild mammals (7, 8), antibiotic treatment is costly, and patients frequently suffer from resurgence of the bacteria (9), vaccination remains the most rational strategy to confer durable protection on populations living in endemic countries and professionals who are frequently exposed to *Brucella*. Unfortunately, there is no available human brucellosis vaccine; all commercially available animal vaccines are live vaccines that would cause disease in humans (10, 11).

The first step in the rational selection of candidate vaccines is to identify immune markers associated with protective immunity. The central role played by the MyD88/IL-12 signaling axis (12–14), IFN-γ–producing CD4$^+$ T cells (15–17), and specific Abs (17) in the protective immune response against *Brucella* has been well established. However, those results were obtained primarily through analysis of the splenic immune response following i.p. infection, and they teach us little about mucosal immune defenses constituting the first barrier protecting the host against brucellosis

*Microorganisms Biology Research Unit (URBM), Laboratory of Immunology and Microbiology, Namur Research Institute for Life Sciences, University of Namur, 5000 Namur, Belgium; [†]Department of Molecular and Cellular Interactions, Flanders Interuniversity Institute for Biotechnology, Free University of Brussels (VUB), 1050 Brussels, Belgium; [‡]Immunologie et Neurogénétique Expérimentales et Moléculaires – UMR7355 CNRS – Université d'Orléans, 45071 Orleans, France; [§]Institute of Infectious Disease and Molecular Medicine, University of Cape Town, Capetown 7925, South Africa; and [¶]Laboratoire de Parasitologie, Faculté de Médecine, Université Libre de Bruxelles, 1070 Bruxelles, Belgium

[1]D.H.M. and A.M. should be considered equally as first authors.

ORCID: 0000-0002-4226-1845 (G.P.).

Received for publication October 23, 2015. Accepted for publication March 3, 2016.

This work was supported by grants from the Fonds National de la Recherche Scientifique (FNRS) (Convention No. 3.4.600.06.F from the Fonds de la Recherche Scientifique Médicale–FNRS, Belgium), and by the Interuniversity Attraction Poles Programme initiated by the Belgian Science Policy Office. E.M. is a Research Associate at the Fonds de la Recherche Scientifique (FRS)–FNRS (Belgium). B.R. was supported by the Agence Nationale pour la Recherche (Agence Nationale de la Recherche 2007/Programme Microbiologie, Immunologie et Maladies Emergentes-103-02), Fondation pour la Recherche Médicale (FRM Allergy DAL 2007 0822007), Fonds Européen de Développement Régional Grant FEDER Asthme 1575-32168, and Le Studium, Orléans. D.H.M. holds Ph.D. grants from the FRS-FNRS (Belgium).

Address correspondence and reprint requests to Dr. Eric Muraille, Laboratoire de Parasitologie, Faculté de Médecine, Université Libre de Bruxelles, Route de Lennik 808, CP 616, 1070 Bruxelles, Belgium. E-mail address: emuraille@hotmail.com

The online version of this article contains supplemental material.

Abbreviations used in this article: HKBr, heat-killed *B. melitensis*; i.n., intranasal(ly); iNOS, inducible NO synthase; mCherry-Br, mCherry-expressing *B. melitensis*; MHCII, MHC class II; p.i., postinfection; RT, room temperature; wt, wild-type.

under natural conditions. Human brucellosis is frequently acquired via aerosol exposure (18), and 10–100 bacteria seem sufficient to infect humans in this manner (19). Aerosol or intranasal (i.n.) exposure of mice (20) or macaques (21) to low (10^2–10^3) doses of virulent *B. melitensis* 16M caused chronic pulmonary infection, followed by systemic infection of the spleen and liver. Interestingly, the TLRs involved in the control of *Brucella* following i.n. infection in mice appear different in the lungs, liver, and spleen (22), suggesting that the nature of the protective immune response may depend on the organ. Therefore, caution is warranted when interpreting the significance of host immune effector components identified previously only via analysis of the spleen.

In the current study, we analyzed the protection levels and immune responses elicited in several compartments (lungs, spleen, liver, and blood) at different times after primary and secondary i.n. infection of C57BL/6 mice with virulent *B. melitensis* 16M. We used a large panel of genetically deficient mice to compare the importance of the IFN-γ–mediated response, the IL-17RA–mediated response, and γ/δ^+ T, α/β^+ T, $CD4^+$ T, $CD8^+$ T, and B cells in the control of primary and secondary *Brucella* infection.

Materials and Methods

Ethics statement

The procedures used in this study and the handling of the mice complied with current European legislation (directive 86/609/EEC) and the corresponding Belgian law "Arrêté royal relatif à la protection des animaux d'expérience du 6 avril 2010 publié le 14 mai 2010." The Animal Welfare Committee of the Université de Namur (Namur, Belgium) reviewed and approved the complete protocol (Permit Number 05-558).

Mice and reagents

Wild-type (wt) C57BL/6 mice were acquired from Harlan (Bicester, U.K.). $IFN\gamma R^{-/-}$ C57BL/6 mice (23), $IL\text{-}12p35^{-/-}$ C57BL/6 mice (24), and $IL12p40^{-/-}$ C57BL/6 mice (25) were acquired from Dr. B. Ryffel (University of Orleans). $IL17RA^{-/-}$ C57BL/6 mice (26) and $IL23p19^{-/-}$ C57BL/6 mice (27) were acquired from Dr. K. Huygen (Belgian Scientific Institute for Public Health, Bruxelles, Belgium). $TAP1^{-/-}$ C57BL/6 mice (28) and $MHCII^{-/-}$ C57BL/6 mice (29) were acquired from Jörg Reimann (University of Ulm, Ulm, Germany). $RAG1^{-/-}$ C57BL/6 mice (30) were acquired from Dr. S. Goriely (Université Libre de Bruxelles). $AID^{-/-}$ C57BL/6 mice (31) were acquired from Dr. H. Jacobs (Netherlands Cancer Institute, Amsterdam, the Netherlands). $TNF\text{-}\alpha^{-/-}$ C57BL/6 (32) and $IL\text{-}6^{-/-}$ C57BL/6 mice (33) were acquired from Dr. C. De Trez (Vrije Universiteit Brussel). $CD3\varepsilon^{-/-}$, $TCR\text{-}\beta^{-/-}$, $TCR\text{-}\delta^{-/-}$, $IL\text{-}1R^{-/-}$, $CCR2^{-/-}$, and $MuMT^{-/-}$ C57BL/6 mice were purchased from The Jackson Laboratory (Bar Harbor, ME). All wt and deficient mice used in this study were bred in the animal facility of the Gosselies campus of the Université Libre de Bruxelles.

We used a wt strain of *Brucella melitensis* 16M and a strain stably expressing a rapidly maturing variant of the red fluorescent protein DsRed (34), the mCherry protein (mCherry-expressing *Brucella melitensis* [mCherry-Br]), under the control of the strong *Brucella* spp. promoter, PsojA. Construction of the mCherry-Br strain was described in detail (35). It was grown in biosafety level III laboratory facilities. Cultures were grown overnight with shaking at 37°C in 2YT medium (Luria-Bertani broth with a double quantity of yeast extract) and washed twice in RPMI 1640 (Life Technologies) (3500 × *g*, 10 min) before inoculation of the mice.

Mice infection

For i.n. infection, mice were anesthetized with a mixture of xylazine (9 mg/kg) and ketamine (36 mg/kg) in PBS before being inoculated i.n. with 2×10^4 CFU wt or mCherry-expressing *B. melitensis* in 30 μl PBS. Control animals were inoculated with the same volume of PBS. The infectious doses were validated by plating serial dilutions of the inoculums. At the selected time postinfection (p.i.), mice were sacrificed by cervical dislocation. Immediately after sacrifice, spleen, liver, and lung cells were collected for bacterial count, flow cytometry, and/or microscopic analyses.

The i.p. infection technique used as a comparison with our i.n. model was described previously (35). Briefly, 2×10^4 CFU wt or mCherry-expressing *B. melitensis* in 500 μl of PBS were injected i.p. without anesthesia.

Antibiotic treatment

Antibiotic treatment was administered to immunized and control mice for 2 wk. The oral treatment was a combination of rifampicin (12 mg/kg) and streptomycin (450 mg/kg) (adapted from Ref. 17) prepared fresh daily and given in the drinking water. To ensure that the antibiotic treatment was effective, some mice from each group were sacrificed 1 wk prior to the challenge, and the CFU counts were evaluated in the spleen.

Anti IL-17A treatment

Neutralizing Abs against IL-17A (clone 17F3) or the recommended isotype control MOPC-21 (Bio X Cell) were administrated by i.p. injection (200 μg/200 μl) 1 h before the i.n. *Brucella* challenge and at 2, 6, and 12 d after the challenge. In addition, to saturate the lungs, mice received 50 μg/20 μl Abs against IL-17A or the isotype control by i.n. inoculation immediately after the i.n. *Brucella* challenge.

Bacterial count

Spleens, livers, and lungs were crushed and transferred to PBS/0.1% Triton X-100 (Sigma-Aldrich). We performed successive serial dilutions in RPMI 1640 to obtain the most accurate bacterial count and plated them onto 2YT medium. The CFU were counted after 5 d of culture at 37°C. For bacterial counts in the blood, 75 μl blood was collected from the tail into heparinized capillary tubes at selected time points and diluted in PBS/0.1% Triton X-100 (Sigma-Aldrich). Serial dilutions were prepared in RPMI 1640 and plated onto 2YT medium. The CFU were counted after 5 d of culture at 37°C.

Cytofluorometric analysis

As described previously (17), spleens were harvested, cut into small pieces, and incubated for 30 min at 37°C with a mix of DNase I fraction IX (Sigma-Aldrich) (100 μg/ml) and 1.6 mg/ml collagenase (400 M and l U/ml). Spleen cells were washed, filtered, and incubated with saturating doses of purified 2.4G2 (anti-mouse FcR; American Type Culture Collection) in 200 μl PBS, 0.2% BSA, and 0.02% NaN3 (FACS buffer) for 20 min at 4°C to prevent Ab binding to the FcR. Various fluorescent mAb combinations in FACS buffer were used to stain 3–5 × 10^6 cells. We acquired the following mAbs from BD Biosciences: FITC-coupled 145-2C11 (anti-CD3ε), FITC-coupled M1/70 (anti-CD11b), FITC-coupled 1A8 (anti-Ly6G), PE-coupled GL3 (anti– TCR-γ/δ), PE-coupled RM4-5 (anti-CD4), PE-coupled 53-6.7 (anti-CD8α), PE-coupled PK136 (anti-NK1.1), biotin-conjugated RB6-8C5 (anti-Gr1), streptavidin PE, allophycocyanin-coupled 1-A/1-E (anti-MHC class II [MHCII]), and allophycocyanin-coupled BM8 (anti-F4/80). The cells were analyzed on a FACSCalibur cytofluorometer. Dead cells and debris were eliminated from the analysis according to size and scatter.

Intracellular cytokine staining

For intracellular staining, spleen cells were incubated after DNase-collagenase treatment for 4 h in RPMI 1640, 10% FCS with 1 μl/ml Golgi Stop (BD Pharmingen) at 37°C, under 5% CO_2. After washing with FACS buffer and staining for cell surface markers, cells were fixed in PBS/1% PFA for 15–20 min at 4°C. They were permeabilized for 30 min using a saponin-based buffer (10× Perm/Wash in FACS buffer; BD Pharmingen) and stained with allophycocyanin-coupled XMG1.2 (anti–IFN-γ; BD Biosciences). After final fixation in PBS/1% PFA, cells were analyzed on a FACSCalibur cytofluorometer. No signal was detectable with isotype controls.

In vitro stimulation of lung and spleen cells

Control and immunized mice were sacrificed, and lung and spleen cells were harvested. Cells were centrifuged and cultured in RPMI 1640 supplemented with 10% FCS, 1% L-glutamine, 1% nonessential amino acids, 1% pyruvate sodium, and 0.1% gentamicin in six-well plates with 10^7 cells/well in a volume of 2 ml. For stimulation, a concentration of 2×10^7 bacteria/ml heat-killed *B. melitensis* (HKBr) or 0.5 μg/ml Con A (Sigma-Aldrich) was used. Cells were incubated for 7 h at 37°C, 5% CO_2. After adding 1 μl/ml Golgi Stop (BD Pharmingen), the incubation was continued for an additional 13 h at 37°C, 5% CO_2. Cells were washed and stained for flow cytometric analysis, as described above.

Immunofluorescence microscopy

Spleens and livers were fixed for 4 h at room temperature (RT) in 2% paraformaldehyde (pH 7.4), washed in PBS, and incubated overnight at 4°C in a 20% PBS-sucrose solution. Lungs were submitted to the same treatment at RT under a vacuum. Tissues were embedded in Tissue-Tek OCT

compound (Sakura) and frozen in liquid nitrogen, and cryostat sections (5 μm) were prepared. For staining, tissue sections were rehydrated in PBS and incubated in a PBS solution containing 1% blocking reagent (Boehringer) for 20 min before incubation overnight in the same type of solution containing any of the following mAbs or reagents: DAPI nucleic acid stain Alexa Fluor 350 or 488 phalloidin (Molecular Probes) to visualize the structure of the organ and Alexa Fluor 647–coupled BM8 (anti-F4/80; Abcam), Alexa Fluor 647–coupled M1/70 (anti-CD11b; Abcam), Alexa Fluor 647–coupled N418 (anti-CD11c; BioLegend), biotin-coupled RB6-8C5 (anti-Gr1; eBioscience), or purified M-19 (anti-NOS2; Santa Cruz Biotechnology) to stain the cells of interest. Incubation with a secondary mAb, Alexa Fluor 488–coupled goat anti-rabbit IgG (Molecular Probes), for 2 h was necessary for the anti-NOS2 mAb. Biotinylated Abs were incubated for 2 h with Alexa Fluor 350 streptavidin. Detection of *Brucella* Ag was performed by incubation overnight with rabbit polyclonal Abs against HKBr (35), followed by incubation for 2 h with Alexa Fluor 488–coupled goat anti-rabbit IgG (Molecular Probes). Slides were mounted in Fluoro-Gel medium (Electron Microscopy Sciences, Hatfield, PA). Labeled tissue sections were visualized with an Axiovert M200 inverted microscope (Zeiss, Jena, Germany) equipped with a high-resolution monochrome camera (AxioCam HR; Zeiss). Images (1384 × 1036 pixels, 0.16 μm/pixel) were acquired sequentially for each fluorochrome with A-Plan 10×/0.25 N.A. and LD Plan-NeoFluar 63×/0.75 N.A. dry objectives and recorded as eight-bit gray-level *.zvi files. At least three slides/organ were analyzed from three animals, and the results are representative of two independent experiments.

ELISA

Specific murine IgM, IgA, IgG1, IgG2a, and IgG3 isotypes were determined by ELISA. Polystyrene plates (Nunc; 269620) were coated with HKBr (107 CFU/ml). After incubation overnight at 4°C, plates were blocked for 2 h at RT with 200 μl PBS–3.65% casein. The plates were incubated overnight at 4°C with 50 μl serial dilutions of the serum in PBS–3.5% casein. Sera from unimmunized mice were used as the negative control. After four washes with PBS, isotype-specific goat anti-mouse HRP conjugates were added (50 μl/well) at the appropriate dilutions (hIgM from Sigma-Aldrich; hIgA from Invitrogen; LO-MG1-13 HRPO, LO-MG2a-9 HRPO, and LO-MG3-13 HRPO from LO-IMEX). Plates were incubated for 2 h at RT and washed four times in PBS before adding 100 μl substrate solution (BD OptEiA) to each well. After 10 min of incubation at RT in the dark, the enzyme reaction was stopped by adding 25 μl/well 2 N H_2SO_4, and absorbance was measured at 450 nm.

Statistical analysis

We used a (Wilcoxon) Mann–Whitney *U* test provided by GraphPad Prism software to analyze our results. Each group of deficient mice was compared with wt mice. The *p* values were considered to represent a significant difference.

Results

Intranasal inoculation leads to slow dissemination of Brucella *in the organism*

The course of *B. melitensis* 16M in wt C57BL/6 mice following i.n. infection was analyzed previously by several research groups (22, 36, 37). However, because the infectious dose, the origin of the mice, and the conditions in the animal facility could influence the course of the infection, we began by establishing the kinetics of infection under our laboratory conditions. Because lungs naturally contain commensal bacteria, we used a mCherry-Br strain of *B. melitensis* 16M displaying kanamycin resistance to evaluate the *Brucella* CFU count during the course of infection.

Following i.n. inoculation with 2×10^4 CFU of *B. melitensis*, wt C57BL/6 mice were sacrificed at 1, 3, 6, 12, 20, 28, and 50 d p.i., and CFU were counted in the lungs, spleen, and liver (Fig. 1A). We observed that bacteria persisted at the same level in the lungs for ∼12 d and then were progressively eliminated. At 28 d p.i., only rare mice displayed detectable CFU in the lungs. The dissemination of *Brucella* from the lungs to the spleen and liver took ∼3 d. From 6 d p.i., the spleen and liver of the majority of mice displayed detectable CFU counts, which peaked at 12–28 d p.i. Infection persisted in the spleen but decreased below the level of detection in the liver of the majority of mice. Compared with i.p. infection with

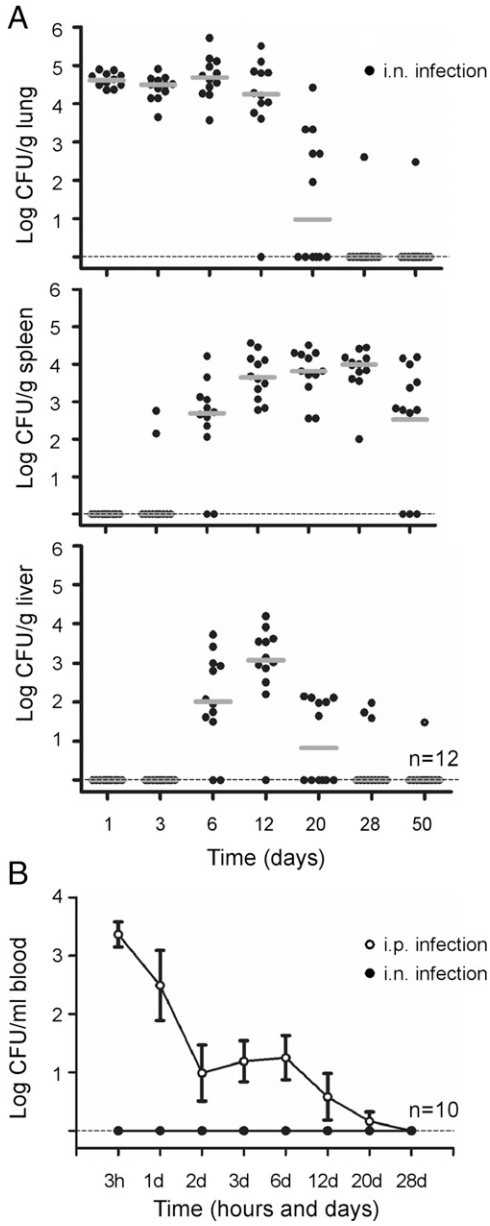

FIGURE 1. Course of *B. melitensis* infection in organs of wt C57BL/6 mice. Mice were inoculated i.n. with 2×10^4 CFU of mCherry–*B. melitensis* and sacrificed at the indicated time points. (**A**) The data represent the number of CFU/g of lungs (*top panel*), spleen (*middle panel*), and liver (*bottom panel*). Horizontal gray lines represent the medians. (**B**) Number of CFU/ml of blood. *n* denotes the number of mice used at each time point. These results are representative of at least three independent experiments.

the same dose of bacteria, a striking characteristic of i.n. infection was the slow dissemination from the primary site of infection to the spleen and liver (38), as well as the absence of detectable bacteria in the bloodstream (Fig. 1B). Because our detection limit was 10 CFU/ml, this result suggests that a very small number of bacteria travel simultaneously in the bloodstream.

After i.n. administration of 2×10^4 CFU, flow cytometry analysis of infected lungs did not reveal a significant modification in the frequency or number of neutrophils ($CD11b^+$ $Ly\text{-}6G^+$ $F4/80^-$), alveolar macrophages ($CD11c^+$ $Ly\text{-}6G^-$ $F4/80^+$), and interstitial macrophages ($CD11c^-$ $Ly\text{-}6G^-$ $F4/80^+$) until 12 d p.i. (data not shown). Intraperitoneal *Brucella* infection induces dense and easily detectable granulomas in the spleen and liver, which primarily contain inducible NO synthase (iNOS)/$NOS2^+$ monocytes and in-

flammatory dendritic cells surrounded by granulocytes (35). All of these cells express high levels of CD11b. Thus, we used iNOS and CD11b markers to detect the presence of aggregates of activated myeloid cells in the lung tissue. We observed (Fig. 2A, data not shown) that lungs of infected mice do not display a greater number of $CD11b^+$ aggregates compared with lungs of control naive mice. In addition, the few $CD11b^+$ aggregates present in the lungs of infected mice are negative for iNOS or the presence of *Brucella* Ags (data not shown). Thus, in agreement with reports by other investigators (39), we conclude that, although nonnegligible CFU levels are reached, *Brucella* lung infection does not lead to granuloma formation during any phase of infection. This suggests that the early control of *Brucella* growth in mucosal lung tissue does not induce or require an inflammatory reaction. To test this hypothesis, we compared the course of *Brucella* infection in wt, IL-$1R^{-/-}$, IL-$6^{-/-}$, TNF-$\alpha^{-/-}$, and $CCR2^{-/-}$ [deficient for monocyte recruitment (40)] C57BL/6 mice (Fig. 3). Mice deficient for IL-1R, IL-6, and TNF-α or the CCR2-dependent recruitment of monocytes displayed CFU counts in the lungs similar to those of wt mice during the first 5 d of infection, confirming that the inflammation process does not seem to be implicated in the early control of *Brucella* infection in the lungs. At 12 and 28 d p.i., only TNF-$\alpha^{-/-}$ mice displayed significantly higher CFU counts in the organs. IL-1R deficiency had a slightly significant impact on the spleen only at 28 d p.i.

In drastic contrast to the lungs, colonization of the spleen (Fig. 2B) and liver (Fig. 2C) was accompanied by $CD11b^+$ $iNOS^+$ granuloma formation. Rabbit polyclonal Abs against HKBr confirm the presence of *Brucella* Ags inside granulomas (Fig. 2D). Unfortunately, the low frequency of *Brucella* in organs does not allow for direct visualization of the bacteria in tissue sections using the mCherry-expressing strain. Interestingly, the location of granulomas in the spleen after i.n. infection was clearly different from their location after i.p. infection. As we reported previously (35), following i.p. infection, granulomas are mainly located in the red pulp during the first days of infection and are found in the white pulp only after 12 d. After i.n. infection, granulomas appear immediately and only inside the marginal zone and white pulp (Fig. 2C), suggesting that the localization of granulomas in the red pulp could be a consequence of the rapid and abrupt infection of the spleen following i.p. injection.

IFN-γR– and IL-17RA–mediated responses contribute to the control of primary i.n. infection

The central role of the TLR4/TLR9/MyD88/IL-12 axis in promoting IFN-γ–producing $CD4^+$ T cells to control *Brucella* growth in the spleen following i.p. infection is well established (14, 16, 35). By comparing the course of i.p. infection in the spleen in wt, IL-$12p35^{-/-}$, IL-$23p19^{-/-}$, and IL-$12p40^{-/-}$ (deficient for both

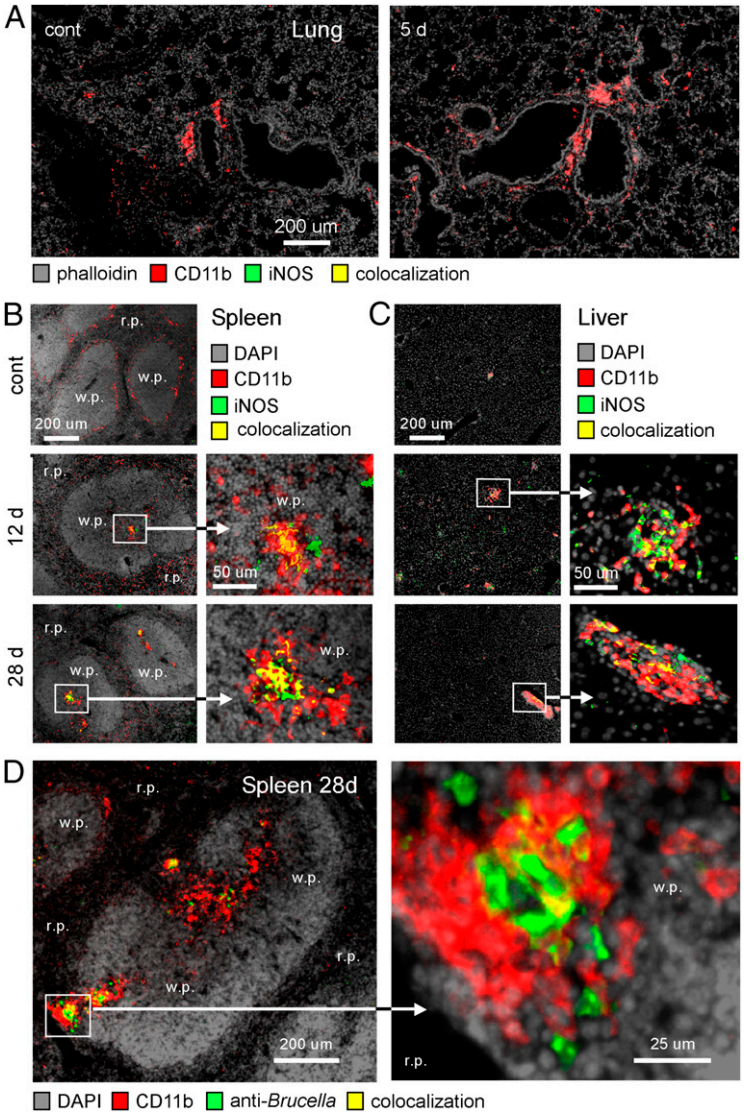

FIGURE 2. $CD11b^+$ granulomas in the spleen and liver of wt C57BL/6 mice. Mice were inoculated i.n. with 2×10^4 CFU of mCherry–*B. melitensis* and sacrificed at the indicated times. Localization by immunofluorescence of $CD11b^+$-, *Brucella* Ag-, and iNOS-expressing cells in the lungs (**A**), spleen (**B** and **D**), and liver (**C**) of naive (cont) and infected mice at the indicated time points. Panels are color-coded with the text for DAPI (nucleus staining), phalloidin (actin staining), or the Ag examined. Data are representative of at least two independent experiments. r.p., red pulp; w.p., white pulp.

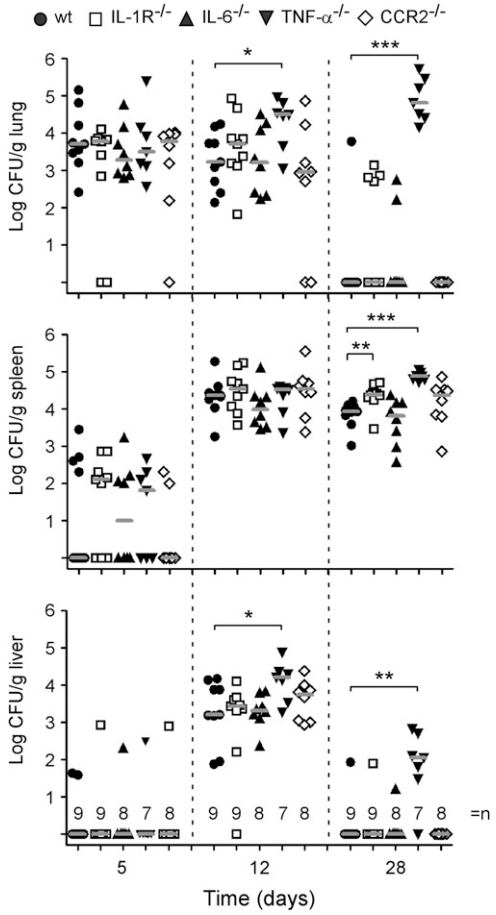

FIGURE 3. Course of *B. melitensis* in organs of wt, IL-1R–deficient, IL-6–deficient, TNF-α–deficient, and CCR2-deficient C57BL/6 mice. wt and deficient mice were inoculated i.n. with 2×10^4 CFU of mCherry–*B. melitensis* and sacrificed at the indicated time points. The data represent the number of CFU/g of lung (*top panel*), spleen (*middle panel*), and liver (*bottom panel*). Horizontal lines represent the medians. *n* denotes the number of mice used for each lineage at each time point. These results are representative of at least two independent experiments. $*p < 0.05$, $**p < 0.01$, $***p < 0.001$.

IL-12 and IL-23) mice, we observed that IL-12p40$^{-/-}$ mice display higher susceptibility than IL-12p35$^{-/-}$ mice, which suggests a weakly compensatory role for IL-23 (affecting the IL-17A–mediated response) in the absence of IL-12p35 (affecting the IFN-γ–mediated response) in the spleen (16). In our i.n. infection model, we analyzed the impact of this deficiency on the control of *Brucella* growth in the lungs, spleen, and liver (Fig. 4A). IL-23p19$^{-/-}$ mice displayed CFU counts similar to wt mice at all time points and in all organs tested. IL-12p35$^{-/-}$ and IL-12p40$^{-/-}$ mice displayed enhanced CFU counts in the spleen throughout the entire course of infection. In drastic contrast to the spleen, IL-12p35 deficiency only had a transient impact on CFU counts in the lungs and liver. At 50 d p.i., these mice eliminated *Brucella* like wt mice. Only IL-12p40 deficiency leads to long-term uncontrolled persistence in the lungs and liver at 50 d p.i. These results demonstrate that the immune requirements for the control of *Brucella* infection are organ-specific and suggest that the IL-23–dependent IL-17A–mediated response may compensate for the partial absence of an IFN-γ–mediated response to control *Brucella* in the lungs and liver.

Then we compared the impact of direct IFN-γR and IL-17RA deficiencies on the course of i.n. *Brucella* infection. As reported previously (41–43), the complete absence of functional IFN-γ signaling leads to high CFU counts in all tested organs (Fig. 4B) and 100% mortality after 35 d p.i. (Fig. 5A). By comparison, the impact of IL-17RA deficiency appears to be limited to higher CFU counts in the lungs during the early stages of infection (Fig. 5), without any associated mortality (data not shown). Interestingly, the impact of IL-17RA deficiency is already pronounced at 5 d p.i. At that point in time, IFN-γR signaling deficiency has no detectable impact in the lungs, suggesting that the IL-17RA–mediated response starts before the IFN-γR–mediated response in the lungs and could constitute the first line of defense against *Brucella* infection.

High mortality in IFN-γR–deficient mice in response to Brucella *infection is associated with dramatic neutrophilia*

The fatal course of *Brucella* infection in all mice displaying a deficiency in IFN-γ signaling [IFN-γ$^{-/-}$ (41, 43), IRF1$^{-/-}$ (42) mice] supports the idea that IFN-γ plays a pivotal role in mediating a protective immune response. However, the absence of mortality in RAG1$^{-/-}$ (16), MyD88$^{-/-}$ (14), and IL-12p35$^{-/-}$ (16) mice is surprising because T cells are described as the main producer of IFN-γ during chronic *Brucella* infection (14, 16), and MyD88 (14) and IL-12p35 (16) have been closely implicated in IFN-γ induction. This shows that mortality results only from the complete absence of IFN-γ and is not proportional to its level. We observed that CFU levels in organs were nearly similar in CD3ε$^{-/-}$ and IFN-γR$^{-/-}$ mice (Fig. 5B), but only IFN-γR$^{-/-}$ mice died (Fig. 5A), suggesting that the lack of control of *Brucella* growth in the organs is not the only reason for IFN-γR deficiency–associated mortality.

To reconcile this enigma, we examined the lungs, spleen, and liver of wt, IL-12p35$^{-/-}$, CD3ε$^{-/-}$, and IFN-γR$^{-/-}$ mice 35 d after i.n. infection by in situ fluorescent microscopy. We observed that only IFN-γR$^{-/-}$ infected mice displayed a dramatic recruitment of Gr1$^+$ cells in tissues (Fig. 6A for lungs, Supplemental Fig. 1 for comparison of the lungs, spleen, and liver). Flow cytometry analysis identified Gr1$^+$ cells in the spleen as neutrophils, as demonstrated by their typical cell surface phenotype: Ly-6G$^+$ F4/80$^-$ MHC-II$^-$ CD11b$^+$ (Supplemental Fig. 2). This dramatic neutrophilia was not correlated with the observation of a higher frequency of IL-17A$^+$ cells by flow cytometry in the spleen of IFN-γR$^{-/-}$ infected mice (data not shown), suggesting that a compensatory IL-17A–mediated response is not implicated in mortality. Interestingly, the IFN-γR deficiency strongly affected the cellular composition of the granulomas in the liver (Fig. 6B) and spleen (data not shown). We showed previously (35) that granulomas induced by *Brucella* infection are primarily composed of iNOS$^+$ monocytes (CD11b$^+$ CD11c$^-$ F4/80^{low}) and inflammatory dendritic cells (CD11b$^+$ CD11c$^+$ F4/80^{high}) with few neutrophils (CD11b$^+$ Ly-6G$^+$/GR1$^+$). We observed a similar cellular composition of the granulomas in the liver (Fig. 6B) and spleen (data not shown) after i.n. infection in wt and IL-12p35$^{-/-}$ mice, with only a partial reduction in iNOS staining in IL-12p35$^{-/-}$ mice. In contrast, IFN-γR$^{-/-}$ infected mice displayed large granulomas dominated by iNOS$^-$ CD11b$^+$ Gr1$^+$ CD11c$^-$ F4/80$^-$ cells. These neutrophil-rich granulomas did not seem able to restrict *Brucella* dissemination because they were correlated with high CFU counts in the blood from all IFN-γR$^{-/-}$ infected mice (Fig. 6C). Note that a kinetic analysis showed that *Brucella* becomes detectable in the blood of IFN-γR$^{-/-}$ mice only starting at 20 d p.i. (data not shown). No bacteria are detected during the course of infection in wt mice (Fig. 1B) and IL-12p35$^{-/-}$ infected mice (data not shown), and only a small fraction of infected CD3$^{-/-}$ mice display a small number of bacteria in the blood (Fig. 6C). As a whole, these results demonstrate that the high

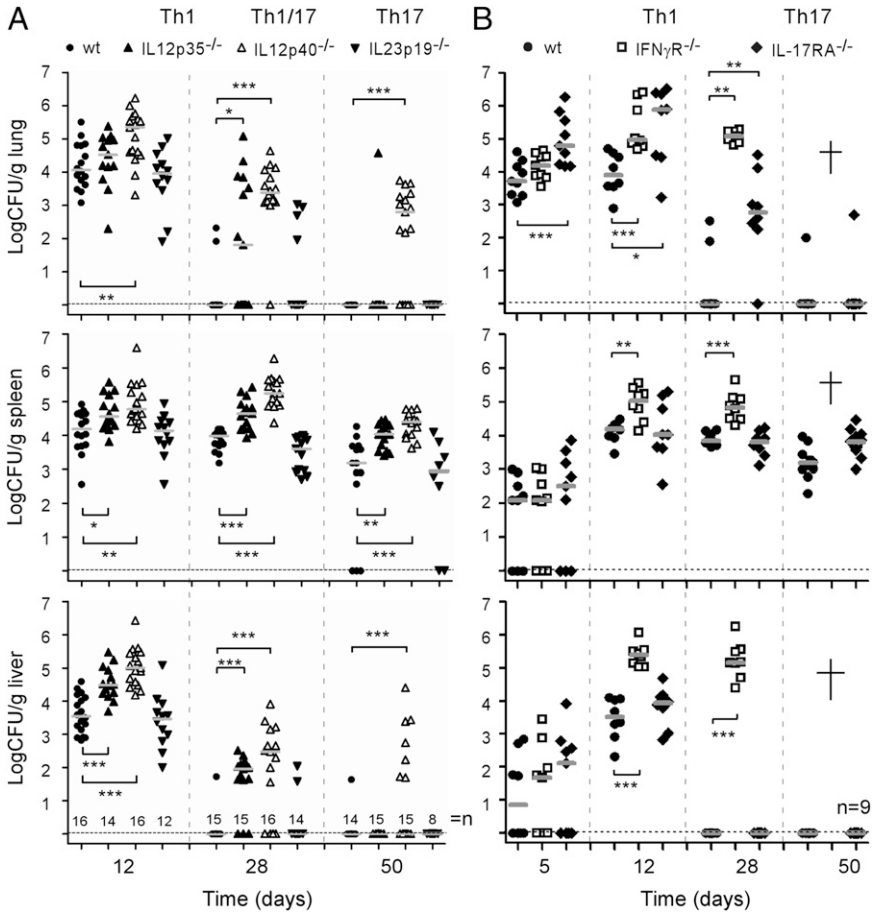

FIGURE 4. Course of *B. melitensis* in organs of wt, IL-12p35–deficient, IL-12p40–deficient, IL-23p19–deficient (**A**), IFN-γR–deficient, and IL-17RA–deficient (**B**) C57BL/6 mice. wt and deficient mice were inoculated i.n. with 2×10^4 CFU of mCherry–*B. melitensis* and sacrificed at the indicated time points. The data represent the number of CFU/g of lung (*top*), spleen (*middle*), and liver (*bottom*). Bars represent the medians. *n* denotes the number of mice used for each lineage at each time point. These results are representative of at least three independent experiments. $*p < 0.05$, $**p < 0.01$, $***p < 0.001$.

mortality observed in IFN-γR$^{-/-}$ mice following *B. melitensis* infection is associated with dramatic neutrophilia leading to multiple organ failure and a major alteration in granuloma formation associated with the persistence of bacteria in the blood.

Contribution of lymphocyte subsets to the control of Brucella *growth after primary i.n. infection*

To determine the lymphocyte populations implicated in the control of primary i.n. *Brucella* infection, we compared the course of infection in various strains of C57BL/6 mice genetically deficient for key genes affecting specific lymphocyte subsets.

The absence of α/β$^+$ or γ/δ$^+$ T lymphocytes leads to a lack of *Brucella* control in the lungs (Fig. 7A). TCR-β deficiency affects early *Brucella* control in the lungs and late control in all organs. In contrast, TCR-δ deficiency strongly impairs early *Brucella* growth in the lungs but has only a transient impact on spleen and liver bacterial loads at 12 d p.i., with no impact on late control at 28 and 50 d p.i. Comparison of TAP1 and MHCII deficiencies (Fig. 7B) suggests that CD8$^+$ α/β$^+$ T lymphocytes only participate in the early control of *Brucella* in the lungs and for a short period of time in the spleen at 28 d p.i. In striking contrast, MHCII deficiency affecting CD4$^+$ α/β$^+$ T lymphocytes fully abrogates *Brucella* control in all organs from 12 to 50 d p.i., thus confirming the crucial role played by CD4$^+$ α/β$^+$ T lymphocytes in the protective immune response against chronic *Brucella* infection (Fig. 7B). Thus, although γ/δ$^+$ T cells and CD8$^+$ α/β$^+$ T cells constitute a first line of defense in mucosal lung tissue, CD4$^+$ α/β$^+$ T cells appear to be involved in the later control of infection in all organs.

Comparison of the cell surface phenotype of IFN-γ–producing cells in the spleen of wt mice following i.p. and i.n. *Brucella* infection showed that CD4$^+$ α/β$^+$ T lymphocytes are the dominant IFN-γ–producing cells at all times during infection (Fig. 8). In contrast to i.p. infection, we did not observe an early peak in IFN-γ–producing γ/δ$^+$ T lymphocytes, NK, or CD8$^+$ α/β$^+$ T lymphocytes during i.n. infection, suggesting that early activation of these cells during i.p. infection could be a consequence of the rapid and massive dissemination of *Brucella* in the spleen.

As we observed previously in an i.p. model (16), the course of *Brucella* infection appears to be similar in the lungs, spleen, and liver of i.n. infected wt, AID$^{-/-}$ (deficient for activation-induced deaminase-mediated isotype switching), and MuMT$^{-/-}$ (deficient for B lymphocytes) C57BL/6 mice at all time points tested (Fig. 9). This demonstrates that Abs do not play a crucial role in the control of primary *Brucella* infection in our i.n. infectious model.

Intranasal Brucella *infection induces protective memory acting in the lung*

To gain further insight into the secondary immune response against *Brucella*, wt mice received i.n. administrations of 30 μl of PBS alone (control mice) or 2×10^4 CFU of the wt (nonfluorescent) strain of *B. melitensis.* At 28 d p.i., both groups were treated daily with a combination of antibiotics (see *Materials and Methods*) for 2 wk to eliminate the *Brucella*. As shown previously (17), this treatment led to the complete elimination of *Brucella* in all tested organs of the infected mice. After a rest period of 2 wk, control mice and previously infected mice were challenged with an mCherry-Br strain of *B. melitensis.* Kinetic analysis of the CFU counts in the lungs, spleen, and liver (Fig. 10A) showed that the previously infected animals displayed a greater ability to control *Brucella* infection. The CFU counts in the lungs had already decreased by >1 log at 6 d. In contrast to primary infected mice, a majority of the secondary infected mice did not display bacteria in the spleen at 12 and 28 d p.i.

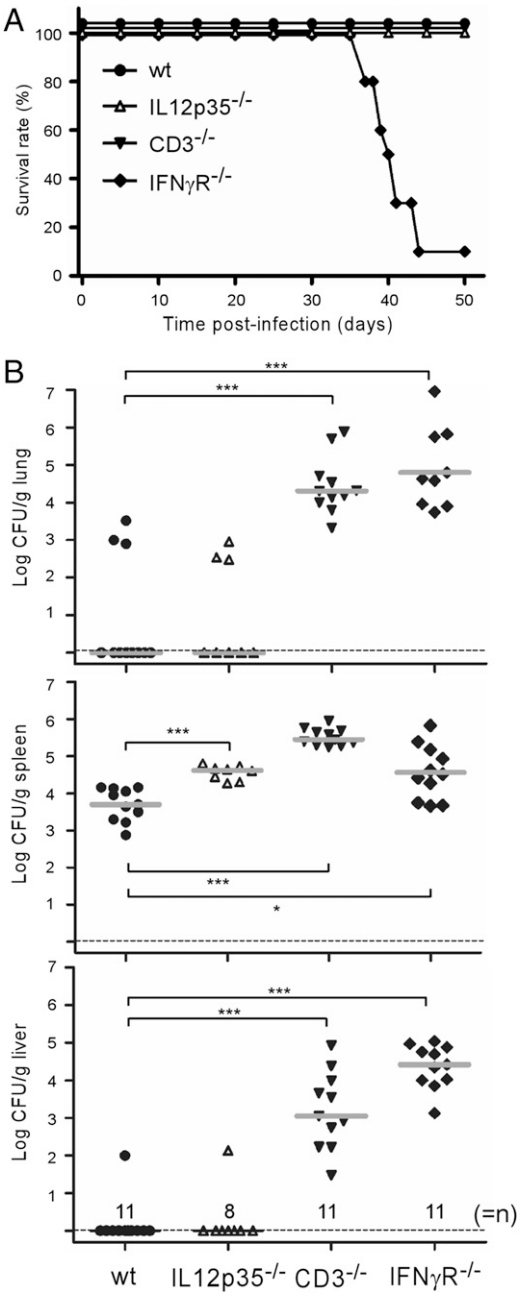

FIGURE 5. Comparison of *B. melitensis* infection among wt, IL12p35-deficient, CD3–deficient, and IFN-γR–deficient C57BL/6 mice. wt and deficient mice were infected i.n. with 2×10^4 CFU of mCherry-*B. melitensis*. (**A**) Survival curve of wt and deficient mice ($n = 10$). (**B**) Infected wt and deficient mice were sacrificed at 35 d p.i. The data represent the number of CFU/g of lung (*top panel*), spleen (*middle panel*), and liver (*bottom panel*). Horizontal gray lines represent the medians. *n* denotes the number of mice used for each lineage. These results are representative of at least two independent experiments. $*p < 0.05$, $***p < 0.001$.

It is interesting to note that i.n. infection protects against i.n. and i.p. challenges (Fig. 10B). On the whole, these results demonstrate that *Brucella* infection induces development in the lung of a protective memory that limits or impairs the dissemination of bacteria from the lung to the spleen and liver.

$CD4^+$ and $CD8^+$ α/β^+ T cells are able to control secondary i.n. Brucella *infection*

Characterization of the lymphocyte populations and Th cell polarization necessary to control secondary mucosal *Brucella* infection constitutes the first step in understanding the underlying mechanisms of the protective immune response and developing a rational strategy to select a protective candidate vaccine against brucellosis. Previous studies by our group using an i.p. *B. melitensis* infectious model with the same *B. melitensis* strain (17) showed that genetic deficiencies leading to a lack of $CD4^+$ T cells ($MHCII^{-/-}$ mice), B cells (MuMT mice), or IL-12 ($IL\text{-}12p35^{-/-}$ mice) completely impaired the ability of mice to develop a protective secondary immune response limiting infection of the spleen.

wt, $CD3\varepsilon^{-/-}$, $TCR\text{-}\beta^{-/-}$, $TCR\text{-}\delta^{-/-}$, $TAP1^{-/-}$, $MHCII^{-/-}$, $MuMT^{-/-}$, $IL\text{-}12p35^{-/-}$, $IL\text{-}17RA^{-/-}$ and $IL\text{-}23p19^{-/-}$ mice infected with wt *B. melitensis* 28 d previously and treated with antibiotics as described previously were challenged with mCherry–*B. melitensis*. Naive wt mice were used as the internal control. Fig. 11 shows the CFU counts in the spleen at 28 d postchallenge. We observed that only the spleen of $CD3\varepsilon^{-/-}$ and $TCR\text{-}\beta^{-/-}$ mice displayed a lack of control of *Brucella* growth compared with wt mice. They were also the only mice to present persisting infection in the lungs following the *Brucella* challenge (data not shown). In striking contrast with an i.p. infection model (17), deficiencies in MHCII, IL-12p35, or B cells do not significantly impair the development of protective immune memory.

The negligible role of B lymphocytes in the control of an i.n. secondary challenge is not due to an impaired ability of i.n. infection–induced specific Abs to control *Brucella*. This is demonstrated by the fact that i.p.– and i.n.–infected mice displayed specific circulating Abs against *Brucella* at 28 d p.i. (Supplemental Fig. 3A) and were equally able to control the bacteria counts in the blood after i.p. challenge with 5×10^7 CFU of *B. melitensis* (Supplemental Fig. 3B).

The efficient control of secondary *Brucella* infection observed in $IL\text{-}12p35^{-/-}$ mice challenges the idea that the IFN-γ–mediated response is crucial to *Brucella* control. To determine whether the IL-17A–mediated response compensates for the lack of the IL-12–dependent IFN-γ–mediated response in $IL\text{-}12p35^{-/-}$ immunized mice, we tested the impact of IL-17A neutralization in these mice. After i.n. challenge, wt and $IL\text{-}12p35^{-/-}$ immunized mice were treated with neutralizing Abs against IL-17A, as indicated in *Materials and Methods*. We observed (Fig. 11B) that this treatment abolishes the protection in $IL\text{-}12p35^{-/-}$ challenged mice but not in wt mice. A similar treatment with the isotype control had no detectable impact (data not shown). Taken together, these results suggest that the IL-17A–mediated response can compensate for the reduced IFN-γ–mediated response in $IL12p35^{-/-}$ mice to control a *Brucella* challenge. Unfortunately, a similar experiment would not be feasible in $IFN\text{-}\gamma R^{-/-}$ mice because the complete absence of the IFN-γ signaling pathway leads to the death of all *Brucella*-infected mice around 35–40 d p.i., even with oral antibiotic treatment (described in *Materials and Methods* section) starting at 20 d and reinforced by i.p. injection of the antibiotic (data not shown).

Finally, to identify the IFN-γ– and IL-17A–producing cells in the lung and spleen during the memory response, we performed a kinetic analysis of the cytokines by flow cytometry in challenged wt mice. In the absence of in vitro restimulation, we did not detect IFN-γ and IL-17A in the lung and spleen cell populations from challenged mice at any time point tested (data not shown), which suggests that the levels of these cytokines are very low in vivo. To solve this problem, we stimulated the lung and spleen cells from control and immunized wt mice overnight in vitro with HKBr or 0.5 μg/ml of Con A (Fig. 12A). HKBr stimulation induces $IFN\text{-}\gamma^+$ cells in the spleen of immunized mice but not control mice. These cells are α/β^+ T cells (Fig. 12B) and mainly $CD4^+$ (data not

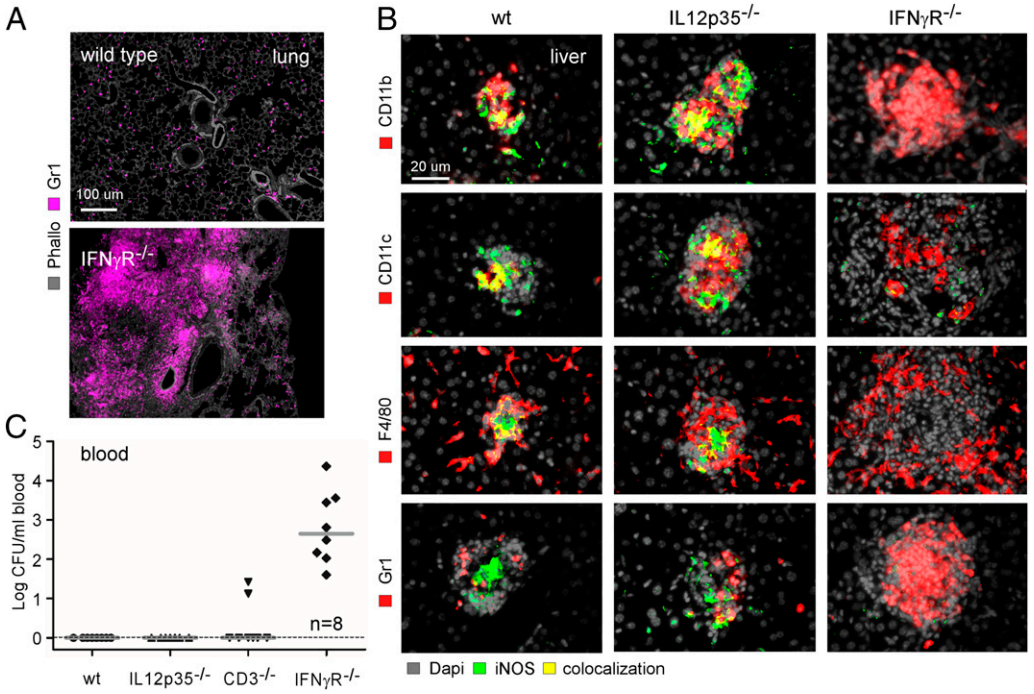

FIGURE 6. Immunofluorescent microscopic analysis of lungs and liver of wt, IL-12p35–deficient, and IFN-γR–deficient C57BL/6 mice. wt, IL-12p35–deficient, CD3-deficient, and IFN-γR–deficient mice were injected i.n. with 2×10^4 CFU of mCherry–*B. melitensis* and sacrificed at 35 d p.i. (**A**) Immunohistofluorescence of lung from wt (*upper panel*) and IFN-γR–deficient mice (*bottom*). Panels are color-coded with the text for phalloidin (actin staining) or the Ag examined (Gr1). (**B**) Phenotypic analysis of granuloma in the liver of infected wt, IL-12p35–deficient, and IFN-γR–deficient mice. Panels are color-coded with the text for DAPI (nucleus staining) or the Ag examined. (**C**) Number of CFU/ml of blood in wt, IL-12p35–deficient, CD3-deficient, and IFN-γR–deficient mice. Horizontal gray line represents the median. *n* denotes the number of mice used for each lineage. Data are representative of at least two independent experiments.

shown). Similar stimulation of lung cells did not lead to detectable IFN-γ production. Unspecific Con A stimulation is required to induce IFN-γ^+ cells in lung cells. These cells also appear to be α/β^+ T cells (Fig. 12B) and mainly $CD4^+$ (data not shown). Lung cells from immunized mice display a higher frequency of IFN-γ^+ cells upon Con A stimulation compared with control mice, sug-

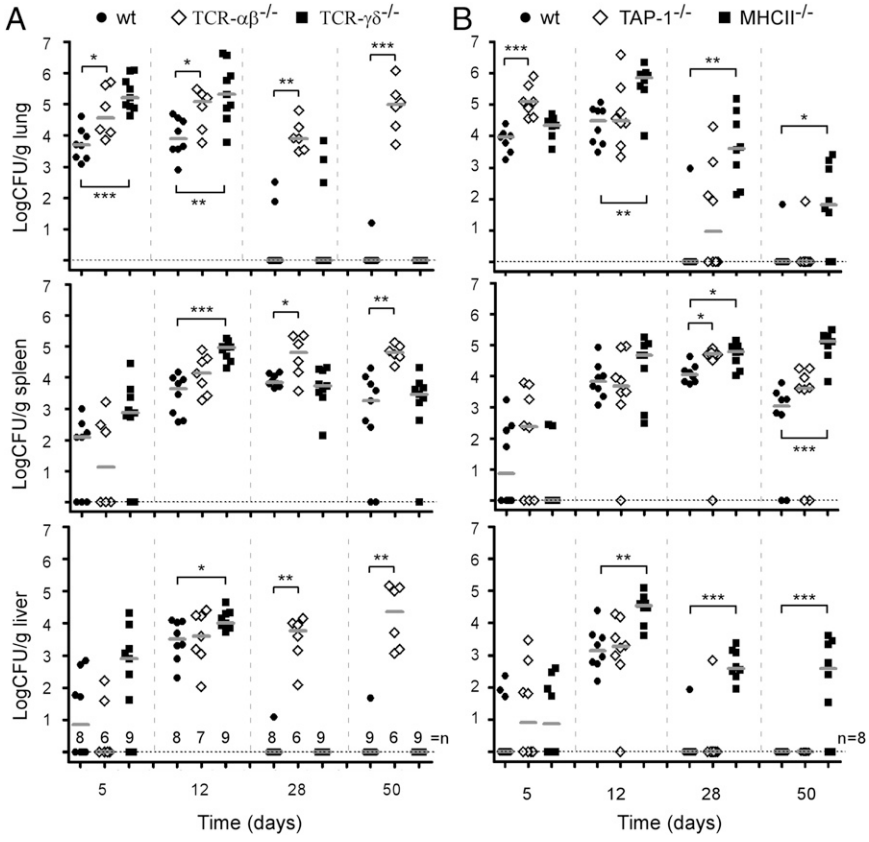

FIGURE 7. Course of *B. melitensis* in organs of wt, TCR-β–deficient, TCR-δ–deficient, TAP1-deficient, and MHCII-deficient C57BL/6 mice. (**A** and **B**) wt and deficient mice were inoculated i.n. with 2×10^4 CFU of mCherry–*B. melitensis* and sacrificed at the indicated time points. The data represent the number of CFU/g of lung (*top panels*), spleen (*middle panels*), and liver (*bottom panels*). Horizontal gray lines represent the medians. *n* denotes the number of mice used for each lineage at each time point. These results are representative of at least three independent experiments. $*p < 0.05$, $**p < 0.01$, $***p < 0.001$.

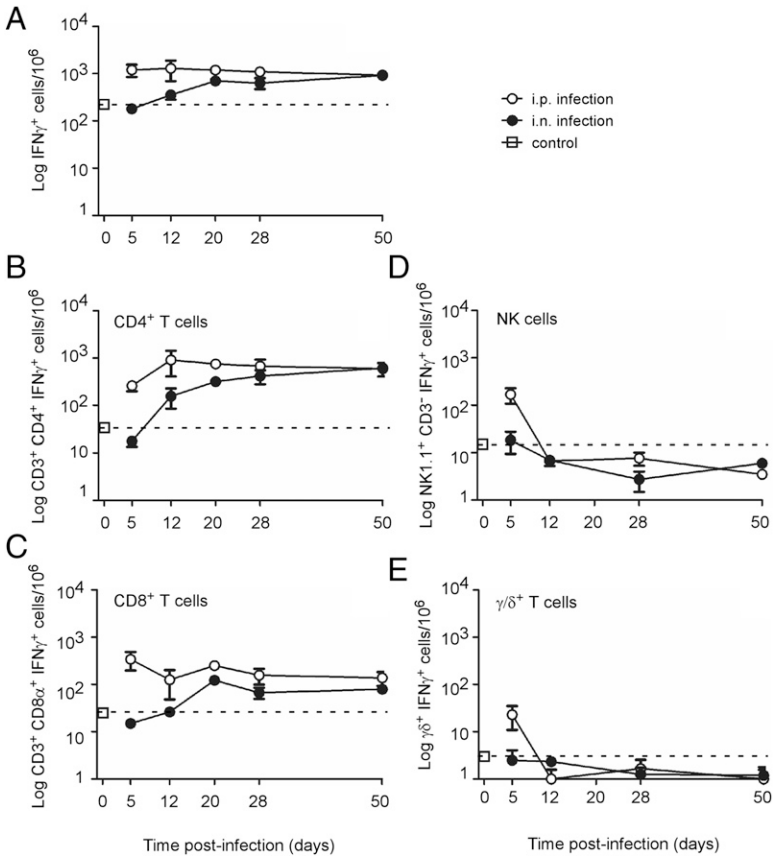

FIGURE 8. IFN-γ production in the spleen of wt C57BL/6 mice after *B. melitensis* infection. wt mice were infected i.n. or i.p. with 2×10^4 CFU of mCherry–*B. melitensis* and sacrificed at the indicated time points. Spleen cells were collected and analyzed by flow cytometry. Cells were gated according to the size and scatter to exclude dead cells and debris for analysis. Number (mean ± SEM) of IFNγ$^+$ cells (**A**), CD3$^+$ CD4$^+$ IFNγ$^+$ cells (**B**), CD3$^+$ CD8$^+$ IFNγ$^+$ cells (**C**), NK1.1$^+$ CD3$^-$ IFNγ$^+$ cells (**D**), and γδ$^+$ IFNγ$^+$ cells (**E**) per 10^6 spleen cells acquired at different times p.i. Squares and dashed lines indicate the level of IFN-γ production by each cell type in naive mice. These results are representative of at least two independent experiments.

gesting that *Brucella* infection induces specific CD4$^+$ α/β$^+$ T cells in the lung. Unfortunately, under the same experimental conditions, we did not detect IL-17A–producing cells in response to HKBr or Con A, suggesting that the frequency of these cells is extremely low or that these cells are lost during the flow cytometry protocol.

A comparison of immune effector mechanisms essential to the control of *Brucella* infection in i.p. and i.n. infection models is shown in Fig. 13.

Discussion

A growing number of clinically relevant infectious diseases are caused by pathogen persistence in the host and require long-lasting and costly therapies (44). Chronic infection is generally the consequence of the ability of a pathogen to escape the adaptive immune response and generate a microenvironment in which it can survive. Therefore, it is crucial to neutralize such pathogens before they disseminate and colonize the host. The major point of entry for many pathogens is the gastrointestinal or respiratory tract, or the genital mucosa (reviewed in Ref. 45), suggesting that mucosal protective immune responses must be induced to counteract pathogen dissemination. However, the ways by which mucosal immunization could generate protective frontline immunity against pathogens remain largely undefined. *Brucella* establishes a stealthy infection in mice and constitutes an interesting experimental model that can be used to analyze the relationships between hosts and intracellular stealth pathogens (46, 47). Although the aerosol route is a common cause of infection in nature (1), a relatively limited number of *Brucella* studies (20, 22, 36, 37, 48, 49) investigated the protective immune response following respiratory infection. In this study, we analyzed the progression of *B. melitensis* in the lungs, spleen, and liver of C57BL/6 mice, as well as the nature of the protective immune response following primary and secondary i.n. infection, and compared them with our results (16, 17, 35, 38) obtained in the classical i.p. infection model.

In contrast to i.p. infection (35, 38), i.n. infection does not lead to the rapid dissemination of *Brucella* in the spleen and liver or to detectable and prolonged persistence of *Brucella* in the blood. This could explain why *Brucella*-induced granulomas in the spleen immediately appeared primarily in the white pulp in this i.n. model and not in the red pulp as previously described following i.p. infection (35). We hypothesize that i.p. infection saturates the marginal zone filter of the spleen consisting of marginal zone macrophages and dendritic cells, thus allowing for the infection of red pulp F4/80$^+$ macrophages. These observations suggest that the route of infection could potentially alter the tissue localization of the bacteria and the phenotype of the primary infected cells.

The cytokines IL-1, IL-6, and TNF-α are sometimes referred to as the inflammatory triad because they are key mediators of local and systemic inflammatory responses. Impaired IL-1 (50, 51), IL-6 (52–54), and TNF-α (55–57) signaling causes enhanced susceptibility of mice to infection with various pathogens. Surprisingly, in our experimental model, we observed that early *Brucella* control in the lungs is not affected by IL-1R, IL-6, or TNF-α deficiency. Furthermore, during the late phase of control, only TNF-α deficiency strongly affected CFU counts of *Brucella* in the organs. In keeping with this observation, *Brucella* was recently shown to induce weak IL-1β, IL-6, and TNF-α production in lung alveolar macrophages compared with peritoneal macrophages (58). The chemokine receptor CCR2 has been implicated in the recruitment of inflammatory monocytes during infection (40). CCR2 deficiency impaired development of a protective immune response in several infectious models (40, 59, 60). We observed that CCR2 deficiency had no impact on the course of *Brucella* infection in the lungs, liver, or spleen at all time points tested. We also did not detect recruitment of inflammatory cells in

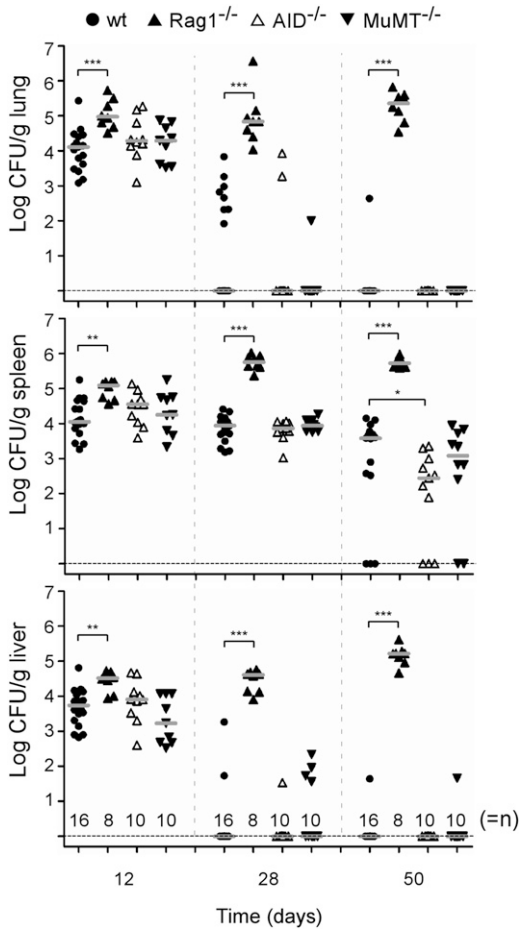

FIGURE 9. Course of *B. melitensis* in organs of wt, RAG1-deficient, AID-deficient, and MuMT-deficient C57BL/6 mice. wt and deficient mice were inoculated i.n. with 2×10^4 CFU of mCherry–*B. melitensis* and sacrificed at the indicated time points. The data represent the number of CFU/g of lung (*top panel*), spleen (*middle panel*), and liver (*bottom panel*). Horizontal gray lines represent the medians. *n* denotes the number of mice used for each lineage at each time point. These results are representative of at least three independent experiments. $*p < 0.05$, $**p < 0.01$, $***p < 0.001$.

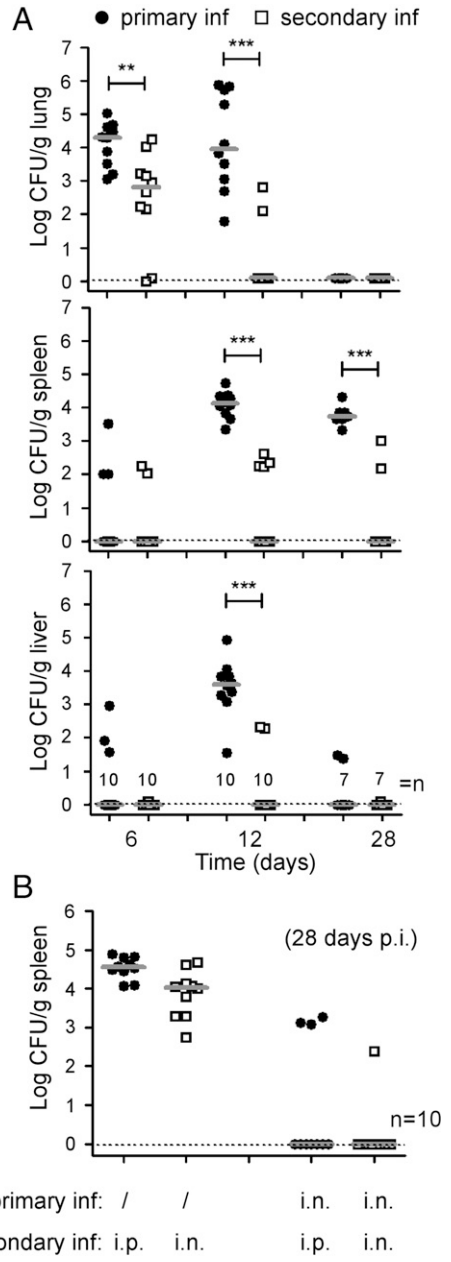

FIGURE 10. Kinetic analysis of the course of infection in wt C57BL/6 mice previously immunized with live *B. melitensis*. wt C57BL/6 mice were immunized i.n. with live *B. melitensis* (2×10^4 CFU) and treated with antibiotics, as described in *Materials and Methods*. (**A**) Naive (primary infected group) and immunized (secondary infected group) wt mice were challenged i.n. with 2×10^4 CFU of mCherry–*B. melitensis* and sacrificed at 6, 12, and 28 d p.i. The data represent the number of CFU/g of lung, spleen and liver. (**B**) Naive and immunized wt mice were challenged i.n. or i.p. with 2×10^4 CFU of mCherry–*B. melitensis* and sacrificed at 28 d postinfection. The data represent the number of CFU/g of spleen. Horizontal gray lines represent the medians. *n* denotes the number of mice used for each lineage at each time point. These results are representative of at least two independent experiments. $**p < 0.01$, $***p < 0.001$.

the lungs during *Brucella* infection by flow cytometry (data not shown) or modification of the cellular organization, such as the formation of granulomas, by microscopy during the period of infection. These results suggest that control of *Brucella* growth in the lungs does not involve the development of a strong local inflammatory response or the recruitment of inflammatory monocytes.

Initially, the IL-17RA–mediated response was primarily associated with the host defense against extracellular pathogens (reviewed in Ref. 61). However, a growing number of recent studies suggest that this response is also involved in the control of intracellular microorganisms, such as *Listeria monocytogenes*, *Salmonella enterica*, and *Mycobacterium tuberculosis* (reviewed in Refs. 62, 63). In the lungs, IL-17A was reported to act primarily on nonhematopoietic cells, such as epithelial cells, endothelial cells, and fibroblasts (reviewed in Ref. 63), to promote the production of numerous proteins with antimicrobial properties and chemokines that attract neutrophils. Although first identified in $CD4^+$ T cells, IL-17A can also be produced by $CD8^+$ T cells and innate cells, such as γ/δ^+ T cells, invariant NKT cells, neutrophils, and innate lymphoid cells (63). There have been few studies of the function of IL-17A–mediated responses in immunity to *Brucella* organisms. In a classical i.p. infection model, we reported that IL-23p19 deficiency, which is known to reduce the IL-17A production response (64), does not significantly affect the control of *Brucella* in the spleen but can partially compensate for IL-12p35 deficiency (16). In the present work, we observed that, following i.n. infection, IL-17RA and IL-23p19 deficiency only had minor effects on CFU counts in the spleen and liver throughout infection. In contrast, IL-17RA$^{-/-}$ mice displayed an important lack of

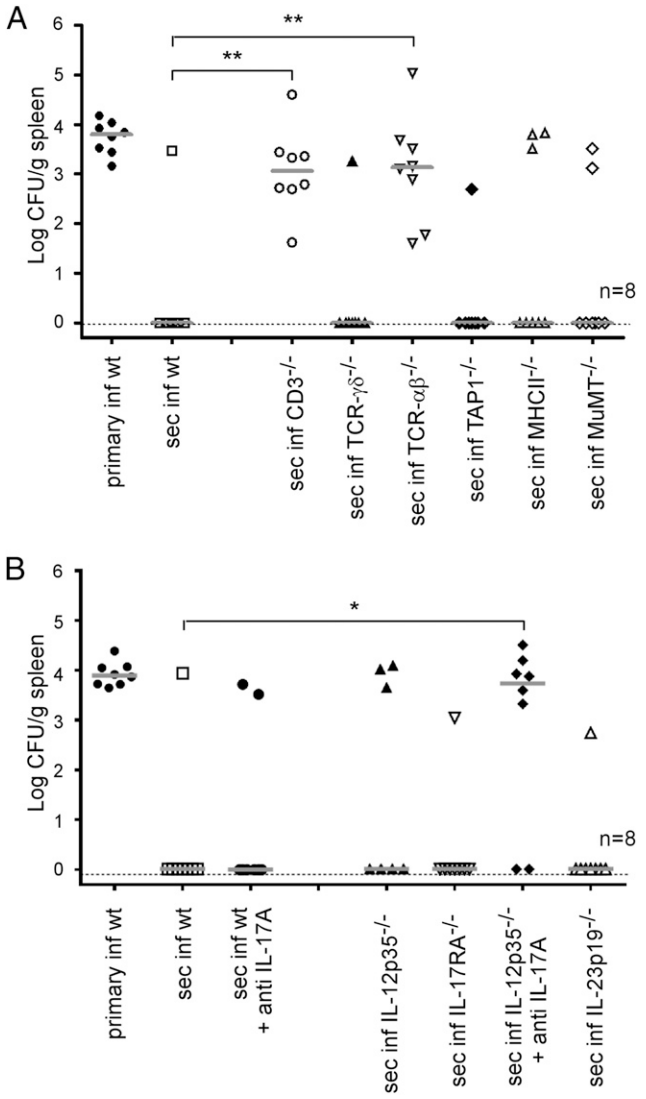

FIGURE 11. Comparison of protection in wt and deficient C57BL/6 mice previously immunized with live *B. melitensis*. wt, CD3$^{-/-}$, TCR-β$^{-/-}$, TCR-δ$^{-/-}$, TAP1$^{-/-}$, MHCII$^{-/-}$, MuMT$^{-/-}$ (**A**), IL-12p35$^{-/-}$, IL-17RA$^{-/-}$, and IL-23p19$^{-/-}$ (**B**) C57BL/6 mice were immunized i.n. with live wt *B. melitensis* (2×10^4 CFU) and treated with antibiotics, as described in *Materials and Methods*. Naive (primary infected group) and immunized (secondary infected group) wt mice were challenged i.n. with 2×10^4 CFU of mCherry–*B. melitensis* and sacrificed at 28 d p.i. Immediately after the challenge, a group of immunized wt and IL-12p35$^{-/-}$ mice was treated with anti–IL-17A, as described in *Materials and Methods*. The data represent the number of CFU/g of spleen. Horizontal gray lines represent the medians. *n* denotes the number of mice used for each lineage at each time point. These results are representative of at least two independent experiments. $*p < 0.05$, $**p < 0.01$.

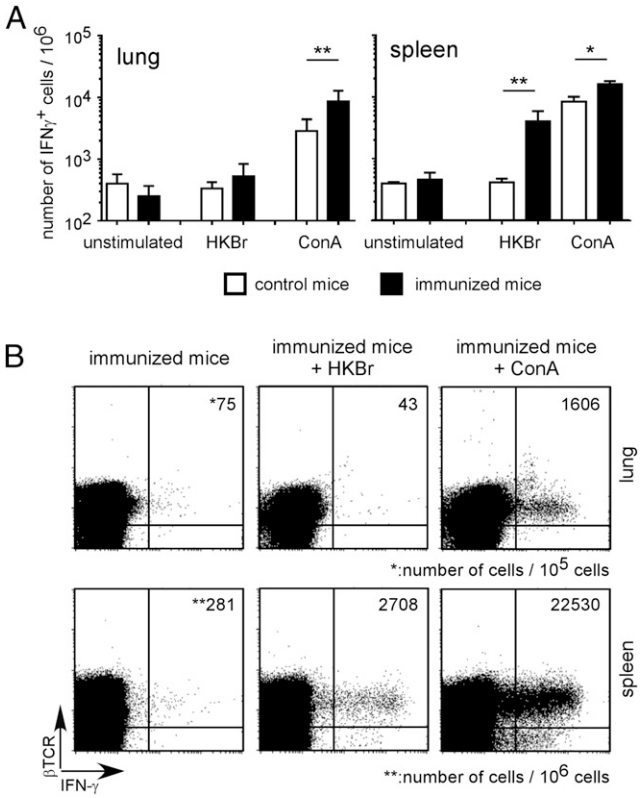

FIGURE 12. In vitro stimulation of lung and spleen cells from wt C57BL/6 mice previously immunized with live *B. melitensis*. wt C57BL/6 mice were injected i.n. with PBS (control mice) or live *B. melitensis* (2×10^4 CFU) (immunized mice) and treated with antibiotics, as described in *Materials and Methods*. Control and immunized mice were sacrificed, and lung and spleen cells were recovered for overnight in vitro stimulation with PBS (unstimulated), 2×10^7 CFU/ml of HKBr, or 0.5 μg/ml of Con A. Cells were analyzed by flow cytometry for TCR-β and IFN-γ expression. (**A**) Mean number of IFN-γ$^+$ cells/10^6 cells acquired. Each data point represents the median value obtained from four individual lungs and spleens. (**B**) Representative TCR-β versus IFN-γ dot plots from lungs and spleens of the group indicated. Numbers represent the number of IFN-γ$^+$ TCR-β$^+$ T cells/10^5 or 10^6 cells acquired, as indicated. The data are representative of two independent experiments. $*p < 0.05$, $**p < 0.01$.

control in the lungs during the early stages of infection, until 12 d p.i. Interestingly, during the same period, IL-23p19 and IFN-γR deficiency had no or only minor effects on CFU counts of *Brucella* in the lungs. These results suggest that the IL-17RA–mediated response constitutes the first line of defense against *Brucella* in the lungs. IL-17A production is generally considered strictly dependent on IL-23, but reduced IL-17A production can still be detected in IL-23p19$^{-/-}$ mice (27). The absence of an effect of IL-23p19 deficiency in our model suggests that low counts of IL-17A could be sufficient to mediate *Brucella* control in the lung. The IFN-γ–mediated response seems to develop late in the lungs, and an IL-17RA–mediated response may compensate for reduced IFN-γ production due to IL-12p35 deficiency, as suggested by the fact that wt and IL-12p35$^{-/-}$ mice, but not IL-12p40$^{-/-}$ mice, control the infection at later stages in the lungs. A similar compensatory phenomenon is observed in the liver. Unfortunately, presumably due to the stealthy nature of *Brucella* infection, we failed to detect IL-17A$^+$ cells in the lungs by flow cytometry and, thus, to identify their source during primary or secondary infection. However, we observed that TCR-δ and TAP1 deficiency, but not MHCII deficiency, also affected early *Brucella* control in the lungs, suggesting that these cells could be a potential source of IL-17A in our model. In keeping with this observation, IL-17 production by γ/δ T cells was reported in a *Brucella* model (65) and in several other pulmonary infectious models (66–68).

Studies carried out in i.p. infectious models clearly established the crucial role of IFN-γ–secreting CD4$^+$ T cells in the primary control of *Brucella* infection (16, 35, 41–43). We confirmed this key role in our i.n. model. From 12 d p.i., IFN-γR and MHCII deficiency led to a dramatic lack of *Brucella* control in the lungs, spleen, and liver. Moreover, we demonstrated that mortality associated with a deficiency in IFN-γ signaling is linked to uncontrolled *Brucella* growth in tissues and probably to severe neutrophilia, which causes multiple organ failure. We failed to

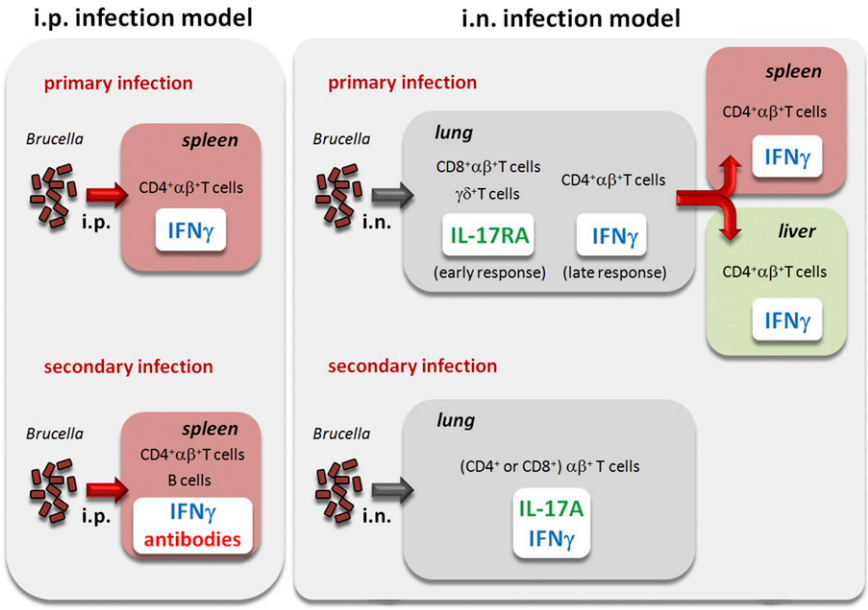

FIGURE 13. Comparison of the i.p. and i.n. *Brucella* infection models. The figure shows the comparison of the immune mechanisms and lymphocyte populations implicated in the control of primary and secondary infection in the i.p. and i.n. infectious models. Note that the identity of the cytokine-producing cells in the lung remains to be determined.

reduce *Brucella*-induced mortality in IFN-γR$^{-/-}$ mice by repeated administration of depleting Abs, such as 1A8 or GR1 specific to neutrophils (data not shown). Most likely, this can be attributed to the chronic nature of *Brucella* infection, which leads to continuous recruitment of new neutrophils. This neutrophilia is not associated with a compensatory IL-17A–mediated response, because we did not detect a higher frequency of IL-17A$^+$ cells in the spleen of infected IFN-γR$^{-/-}$ mice by flow cytometry compared with infected wt mice (data not shown). Likewise, cutaneous and musculoskeletal inflammation observed following i.p. *Brucella* infection in IFN-γ$^{-/-}$ mice is independent of the Th17 response (69). In an *Ehrlichia muris* infection model (70), IFN-γ was shown to control infection by directly promoting the differentiation of myeloid cells into monocytes. In the absence of IFN-γ signaling, *E. muris* infection only promotes the expansion of neutrophils, which do not play a protective role during *Brucella* infection (71) and are generally associated with massive tissue damage, particularly in the lungs (reviewed in Ref. 72). In our i.n. infectious model, the absence of IFN-γR was associated with a drastic alteration in the granuloma composition, which appeared to primarily contain neutrophils, and a lack of tissue confinement of *Brucella*, as demonstrated by the high levels of bacteria observed in the blood of IFN-γR$^{-/-}$ mice during chronic infection but not during the early phases of infection. In summary, our results strongly suggest that the protective role of IFN-γ against *Brucella* infection is primarily limited to the chronic phase of infection and may even have been overestimated based on the exceptional mortality associated with IFN-γ deficiency (41, 43). IFN-γ is clearly crucial to late *Brucella* control in all organs, but is not sufficient, because we observed, in an i.p. infection model (16), that a similar frequency of IFN-γ–producing CD8$^+$ T cells does not replace IFN-γ–producing CD4$^+$ T cells to control *Brucella* growth in the spleen following primary infection.

To identify potential protective immune markers to select candidate vaccines against brucellosis, we previously attempted to characterize the cells and signaling pathways involved in the generation of a protective immune memory response following i.p. priming with live *B. melitensis* (17). We showed that IL-12p35, MHCII, and B cell deficiency completely impair the control of secondary *Brucella* infection in the spleen. Using a similar approach in the i.n. infection model, we analyzed the course of secondary *B. melitensis* infection. Secondary infections appear to be primarily controlled in the lung, because the majority of immunized mice displayed a 10-fold reduction in CFU counts in the lungs at 6 d p.i. compared with primary infected mice, and 60% presented no detectable bacteria in the spleen or liver at 12 d. Using genetically deficient mice, we observed that CD3 and TCR-β deficiency, but not TCR-δ or B cell deficiency, completely abrogates protection in the spleen, thus demonstrating that α/β$^+$ T cells constitute the core of the adaptive immune system implicated in protective immunity against *Brucella*. Because the selective absence of CD4$^+$ α/β$^+$ T cells (in MHCII$^{-/-}$ mice) or CD8$^+$ α/β$^+$ T cells (in TAP1$^{-/-}$ mice) does not affect the efficacy of the secondary protective immune response, we conclude that these two populations are equally able to mediate protective immune responses against an i.n. *Brucella* challenge. Thus, although *Brucella* display immune escape mechanisms that affect CD8$^+$ T cell activity (73, 74), memory CD8$^+$ T cells seem to be able to compensate for the absence of memory CD4$^+$ T cells and, thus, to control secondary i.n. infection with *Brucella*. We also observed that IL-12p35, IL-17RA, and IL-23p19 deficiency did not significantly affect protective immunity against secondary i.n. infection. However, protection in IL-12p35$^{-/-}$ mice is completely abolished by injecting neutralizing IL-17A–specific Abs, which suggests that the IL-17A–mediated response is able to compensate for the reduced IFN-γ–mediated response in IL-12p35$^{-/-}$ mice. In keeping with this observation, live oral brucellosis vaccines were reported to stimulate IFN-γ–mediated and IL-17A–mediated responses in mice (75). Oral immunization with attenuated Δ*znuA* and RB51 strains of *B. melitensis* induces protection in IFNγ$^{-/-}$ BALB/c mice against an i.n. challenge with a virulent *B. melitensis* strain. Neutralization of IL-17A in IFNγ$^{-/-}$ mice reduces the protection conferred by the RB51, but not by the Δ*znuA*, vaccine strain. Thus, the control of secondary i.n. *Brucella* infection seems to be characterized by a redundancy of protective immune mechanisms and, consequently, a great robustness to selective deficiencies of IL-17A–mediated and IFN-γ–mediated response or T cell subsets (γ/δ$^+$ T cells, CD4$^+$ α/β$^+$ T cells, CD8$^+$ α/β$^+$ T cells).

We observed previously (38) that, following i.p. inoculation, *Brucella* display a brief extracellular phase in the blood and then are able to invade erythrocytes and to persist for several weeks in

the bloodstream. Circulating specific Abs present in immunized mice are able to neutralize *Brucella* before erythrocyte invasion and, thus, to reduce *Brucella* dissemination to organs (38). Surprisingly, we observed that protective immunity against an i.n. challenge is not significantly affected by a B cell deficiency. We hypothesize that, following i.n. infection, *Brucella* disseminate from lung tissue inside myeloid phagocytic cells and, thus, avoid neutralizing Abs, a result that is in keeping with the observation that *Brucella* are rapidly found in dendritic cells and alveolar macrophages in lung-draining lymph nodes following primary i.n. infection (39). Thus, the control of i.n. *Brucella* infection appears to be primarily dependent on cellular immunity and independent of humoral immunity.

As a whole, our work highlights the importance of analyzing the protective immune response in experimental models using natural routes of infection. By comparing i.p. and i.n. infection models, we have shown that the location of bacteria in organs and the effector immune mechanisms required to control primary and secondary infection are strongly dependent on the route of inoculation (summarized in Fig. 13). Our results challenge the idea that the Th1 response mediated by $CD4^+$ T cells is indispensable to the development of a protective memory response against *Brucella* infection. In our i.n. infection model, we found that $CD8^+$ T cells may compensate for the absence of $CD4^+$ T cells and control secondary *Brucella* infection. Similarly, a reduced IFN-γ–mediated response can be compensated for by an IL-17A–mediated response. The precise effector mechanisms implicated in these responses remain to be clarified, but our work opens up new areas for future investigations. These findings could improve our ability to develop protective vaccines or therapeutic treatments against brucellosis or other infectious diseases caused by intracellular bacteria. Because cellular immunity only develops following the administration of live bacteria (17), live attenuated vaccines or inactivated, yet metabolically active, bacteria seem to remain the easiest and most potent tools for the production of candidate protective vaccines against brucellosis.

Acknowledgments

We thank Dr. S. Goriely and Dr. Heinz Jacobs for providing $RAG1^{-/-}$ C57BL/6 mice and $AID^{-/-}$ C57BL/6 mice, respectively.

Disclosures

The authors have no financial conflicts of interest.

References

1. Godfroid, J., A. Cloeckaert, J. P. Liautard, S. Kohler, D. Fretin, K. Walravens, B. Garin-Bastuji, and J. J. Letesson. 2005. From the discovery of the Malta fever's agent to the discovery of a marine mammal reservoir, brucellosis has continuously been a re-emerging zoonosis. *Vet. Res.* 36: 313–326.
2. Martirosyan, A., and J.-P. Gorvel. 2013. *Brucella* evasion of adaptive immunity. *Future Microbiol.* 8: 147–154.
3. Colmenero, J. D., J. M. Reguera, F. Martos, D. Sánchez-De-Mora, M. Delgado, M. Causse, A. Martín-Farfán, and C. Juárez. 1996. Complications associated with *Brucella melitensis* infection: a study of 530 cases. [Published erratum appears in *Medicine (Baltimore)* 76: 139.] *Medicine (Baltimore)* 75: 195–211.
4. Pappas, G., P. Papadimitriou, N. Akritidis, L. Christou, and E. V. Tsianos. 2006. The new global map of human brucellosis. *Lancet Infect. Dis.* 6: 91–99.
5. Seleem, M. N., S. M. Boyle, and N. Sriranganathan. 2010. Brucellosis: a re-emerging zoonosis. *Vet. Microbiol.* 140: 392–398.
6. Pappas, G., P. Panagopoulou, L. Christou, and N. Akritidis. 2006. *Brucella* as a biological weapon. *Cell. Mol. Life Sci.* 63: 2229–2236.
7. Zheludkov, M. M., and L. E. Tsirelson. 2010. Reservoirs of *Brucella* infection in nature. *Biol. Bull.* 37: 709–715.
8. Grégoire, F., B. Mousset, D. Hanrez, C. Michaux, K. Walravens, and A. Linden. 2012. A serological and bacteriological survey of brucellosis in wild boar (*Sus scrofa*) in Belgium. *BMC Vet. Res.* 8: 80.
9. Solera, J., E. Martínez-Alfaro, A. Espinosa, M. L. Castillejos, P. Geijo, and M. Rodríguez-Zapata. 1998. Multivariate model for predicting relapse in human brucellosis. *J. Infect.* 36: 85–92.
10. Ficht, T. A., M. M. Kahl-McDonagh, A. M. Arenas-Gamboa, and A. C. Rice-Ficht. 2009. Brucellosis: the case for live, attenuated vaccines. *Vaccine* 27(Suppl. 4): D40–D43.
11. Oliveira, S. C., G. H. Giambartolomei, and J. Cassataro. 2011. Confronting the barriers to develop novel vaccines against brucellosis. *Expert Rev. Vaccines* 10: 1291–1305.
12. Macedo, G. C., D. M. Magnani, N. B. Carvalho, O. Bruna-Romero, R. T. Gazzinelli, and S. C. Oliveira. 2008. Central role of MyD88-dependent dendritic cell maturation and proinflammatory cytokine production to control *Brucella abortus* infection. *J. Immunol.* 180: 1080–1087.
13. Weiss, D. S., K. Takeda, S. Akira, A. Zychlinsky, and E. Moreno. 2005. MyD88, but not toll-like receptors 4 and 2, is required for efficient clearance of *Brucella abortus*. *Infect. Immun.* 73: 5137–5143.
14. Copin, R., P. De Baetselier, Y. Carlier, J.-J. Letesson, and E. Muraille. 2007. MyD88-dependent activation of B220-CD11b+LY-6C+ dendritic cells during *Brucella melitensis* infection. *J. Immunol.* 178: 5182–5191.
15. Zhan, Y., and C. Cheers. 1993. Endogenous gamma interferon mediates resistance to *Brucella abortus* infection. *Infect. Immun.* 61: 4899–4901.
16. Vitry, M.-A., C. De Trez, S. Goriely, L. Dumoutier, S. Akira, B. Ryffel, Y. Carlier, J.-J. Letesson, and E. Muraille. 2012. Crucial role of gamma interferon-producing CD4+ Th1 cells but dispensable function of CD8+ T cell, B cell, Th2, and Th17 responses in the control of *Brucella melitensis* infection in mice. *Infect. Immun.* 80: 4271–4280.
17. Vitry, M.-A., D. Hanot Mambres, C. De Trez, S. Akira, B. Ryffel, J.-J. Letesson, and E. Muraille. 2014. Humoral immunity and CD4+ Th1 cells are both necessary for a fully protective immune response upon secondary infection with *Brucella melitensis*. *J. Immunol.* 192: 3740–3752.
18. Kaufmann, A. F., M. D. Fox, J. M. Boyce, D. C. Anderson, M. E. Potter, W. J. Martone, and C. M. Patton. 1980. Airborne spread of brucellosis. *Ann. N. Y. Acad. Sci.* 353: 105–114.
19. Bossi, P., A. Tegnell, A. Baka, F. Van Loock, J. Hendriks, A. Werner, H. Maidhof, and G. Gouvras. 2004. Bichat guidelines for the clinical management of brucellosis and bioterrorism-related brucellosis. *Euro Surveill.* 9: E15–E16.
20. Henning, L. N., K. T. Gillum, D. A. Fisher, R. E. Barnewall, R. T. Krile, M. S. Anderson, M. J. Ryan, and R. L. Warren. 2012. The pathophysiology of inhalational brucellosis in BALB/c mice. *Sci. Rep.* 2: 495.
21. Mense, M. G., R. H. Borschel, C. L. Wilhelmsen, M. L. Pitt, and D. L. Hoover. 2004. Pathologic changes associated with brucellosis experimentally induced by aerosol exposure in rhesus macaques (*Macaca mulatta*). *Am. J. Vet. Res.* 65: 644–652.
22. Pei, J., X. Ding, Y. Fan, A. Rice-Ficht, and T. A. Ficht. 2012. Toll-like receptors are critical for clearance of *Brucella* and play different roles in development of adaptive immunity following aerosol challenge in mice. *Front. Cell. Infect. Microbiol.* 2: 115.
23. Huang, S., W. Hendriks, A. Althage, S. Hemmi, H. Bluethmann, R. Kamijo, J. Vilcek, R. M. Zinkernagel, and M. Aguet. 1993. Immune response in mice that lack the interferon-gamma receptor. *Science* 259: 1742–1745.
24. Carrera, L., R. T. Gazzinelli, R. Badolato, S. Hieny, W. Muller, R. Kuhn, and D. L. Sacks. 1996. *Leishmania* promastigotes selectively inhibit interleukin 12 induction in bone marrow-derived macrophages from susceptible and resistant mice. *J. Exp. Med.* 183: 515–526.
25. Magram, J., S. E. Connaughton, R. R. Warrier, D. M. Carvajal, C. Y. Wu, J. Ferrante, C. Stewart, U. Sarmiento, D. A. Faherty, and M. K. Gately. 1996. IL-12-deficient mice are defective in IFN γ production and type 1 cytokine responses. *Immunity* 4: 471–481.
26. Nakae, S., Y. Komiyama, A. Nambu, K. Sudo, M. Iwase, I. Homma, K. Sekikawa, M. Asano, and Y. Iwakura. 2002. Antigen-specific T cell sensitization is impaired in IL-17-deficient mice, causing suppression of allergic cellular and humoral responses. *Immunity* 17: 375–387.
27. Ghilardi, N., N. Kljavin, Q. Chen, S. Lucas, A. L. Gurney, and F. J. De Sauvage. 2004. Compromised humoral and delayed-type hypersensitivity responses in IL-23-deficient mice. *J. Immunol.* 172: 2827–2833.
28. Van Kaer, L., P. G. Ashton-Rickardt, H. L. Ploegh, and S. Tonegawa. 1992. TAP1 mutant mice are deficient in antigen presentation, surface class I molecules, and CD4-8+ T cells. *Cell* 71: 1205–1214.
29. Cosgrove, D., D. Gray, A. Dierich, J. Kaufman, M. Lemeur, C. Benoist, and D. Mathis. 1991. Mice lacking MHC class II molecules. *Cell* 66: 1051–1066.
30. Mombaerts, P., J. Iacomini, R. S. Johnson, K. Herrup, S. Tonegawa, and V. E. Papaioannou. 1992. RAG-1-deficient mice have no mature B and T lymphocytes. *Cell* 68: 869–877.
31. Muramatsu, M., K. Kinoshita, S. Fagarasan, S. Yamada, Y. Shinkai, and T. Honjo. 2000. Class switch recombination and hypermutation require activation-induced cytidine deaminase (AID), a potential RNA editing enzyme. *Cell* 102: 553–563.
32. Marino, M. W., A. Dunn, D. Grail, M. Inglese, Y. Noguchi, E. Richards, A. Jungbluth, H. Wada, M. Moore, B. Williamson, et al. 1997. Characterization of tumor necrosis factor-deficient mice. *Proc. Natl. Acad. Sci. USA* 94: 8093–8098.
33. Poli, V., R. Balena, E. Fattori, A. Markatos, M. Yamamoto, H. Tanaka, G. Ciliberto, G. A. Rodan, and F. Costantini. 1994. Interleukin-6 deficient mice are protected from bone loss caused by estrogen depletion. *EMBO J.* 13: 1189–1196.
34. Shaner, N. C., R. E. Campbell, P. A. Steinbach, B. N. G. Giepmans, A. E. Palmer, and R. Y. Tsien. 2004. Improved monomeric red, orange and yellow fluorescent proteins derived from *Discosoma* sp. red fluorescent protein. *Nat. Biotechnol.* 22: 1567–1572.
35. Copin, R., M.-A. Vitry, D. Hanot Mambres, A. Machelart, C. De Trez, J.-M. Vanderwinden, S. Magez, S. Akira, B. Ryffel, Y. Carlier, et al. 2012. In situ microscopy analysis reveals local innate immune response developed around *Brucella* infected cells in resistant and susceptible mice. *PLoS Pathog.* 8: e1002575.

36. Izadjoo, M. J., Y. Polotsky, M. G. Mense, A. K. Bhattacharjee, C. M. Paranavitana, T. L. Hadfield, and D. L. Hoover. 2000. Impaired control of *Brucella melitensis* infection in Rag1-deficient mice. *Infect. Immun.* 68: 5314–5320.
37. Mense, M. G., L. L. Van De Verg, A. K. Bhattacharjee, J. L. Garrett, J. A. Hart, L. E. Lindler, T. L. Hadfield, and D. L. Hoover. 2001. Bacteriologic and histologic features in mice after intranasal inoculation of *Brucella melitensis*. *Am. J. Vet. Res.* 62: 398–405.
38. Vitry, M.-A., D. Hanot Mambres, M. Deghelt, K. Hack, A. Machelart, F. Lhomme, J.-M. Vanderwinden, M. Vermeersch, C. De Trez, D. Pérez-Morga, et al. 2014. *Brucella melitensis* invades murine erythrocytes during infection. *Infect. Immun.* 82: 3927–3938.
39. Archambaud, C., S. P. Salcedo, H. Lelouard, E. Devilard, B. de Bovis, N. Van Rooijen, J. P. Gorvel, and B. Malissen. 2010. Contrasting roles of macrophages and dendritic cells in controlling initial pulmonary *Brucella* infection. *Eur. J. Immunol.* 40: 3458–3471.
40. Kurihara, T., G. Warr, J. Loy, and R. Bravo. 1997. Defects in macrophage recruitment and host defense in mice lacking the CCR2 chemokine receptor. *J. Exp. Med.* 186: 1757–1762.
41. Murphy, E. A., J. Sathiyaseelan, M. A. Parent, B. Zou, and C. L. Baldwin. 2001. Interferon-gamma is crucial for surviving a *Brucella abortus* infection in both resistant C57BL/6 and susceptible BALB/c mice. *Immunology* 103: 511–518.
42. Ko, J., A. Gendron-Fitzpatrick, and G. A. Splitter. 2002. Susceptibility of IFN regulatory factor-1 and IFN consensus sequence binding protein-deficient mice to brucellosis. *J. Immunol.* 168: 2433–2440.
43. Brandão, A. P., F. S. Oliveira, N. B. Carvalho, L. Q. Vieira, V. Azevedo, G. C. Macedo, and S. C. Oliveira. 2012. Host susceptibility to *Brucella abortus* infection is more pronounced in IFN-γ knockout than IL-12/β2-microglobulin double-deficient mice. *Clin. Dev. Immunol.* 2012: 589494.
44. Nugent, R. 2008. Chronic diseases in developing countries: health and economic burdens. *Ann. N. Y. Acad. Sci.* 1136: 70–79.
45. Belyakov, I. M., and J. D. Ahlers. 2009. What role does the route of immunization play in the generation of protective immunity against mucosal pathogens? *J. Immunol.* 183: 6883–6892.
46. Martirosyan, A., E. Moreno, and J. P. Gorvel. 2011. An evolutionary strategy for a stealthy intracellular *Brucella* pathogen. *Immunol. Rev.* 240: 211–234.
47. Fabrik, I., A. Härtlova, P. Rehulka, and J. Stulik. 2013. Serving the new masters - dendritic cells as hosts for stealth intracellular bacteria. *Cell. Microbiol.* 15: 1473–1483.
48. Kahl-McDonagh, M. M., A. M. Arenas-Gamboa, and T. A. Ficht. 2007. Aerosol infection of BALB/c mice with *Brucella melitensis* and *Brucella abortus* and protective efficacy against aerosol challenge. *Infect. Immun.* 75: 4923–4932.
49. Bhattacharjee, A. K., L. Van de Verg, M. J. Izadjoo, L. Yuan, T. L. Hadfield, W. D. Zollinger, and D. L. Hoover. 2002. Protection of mice against brucellosis by intranasal immunization with *Brucella melitensis* lipopolysaccharide as a noncovalent complex with *Neisseria meningitidis* group B outer membrane protein. *Infect. Immun.* 70: 3324–3329.
50. Verdrengh, M., J. A. Thomas, and O. H. Hultgren. 2004. IL-1 receptor-associated kinase 1 mediates protection against *Staphylococcus aureus* infection. *Microbes Infect.* 6: 1268–1272.
51. Reiniger, N., M. M. Lee, F. T. Coleman, C. Ray, D. E. Golan, and G. B. Pier. 2007. Resistance to *Pseudomonas aeruginosa* chronic lung infection requires cystic fibrosis transmembrane conductance regulator-modulated interleukin-1 (IL-1) release and signaling through the IL-1 receptor. *Infect. Immun.* 75: 1598–1608.
52. Dalrymple, S. A., L. A. Lucian, R. Slattery, T. McNeil, D. M. Aud, S. Fuchino, F. Lee, and R. Murray. 1995. Interleukin-6-deficient mice are highly susceptible to *Listeria monocytogenes* infection: correlation with inefficient neutrophilia. *Infect. Immun.* 63: 2262–2268.
53. Dalrymple, S. A., R. Slattery, D. M. Aud, M. Krishna, L. A. Lucian, and R. Murray. 1996. Interleukin-6 is required for a protective immune response to systemic *Escherichia coli* infection. *Infect. Immun.* 64: 3231–3235.
54. Jebbari, H., C. W. Roberts, D. J. Ferguson, H. Bluethmann, and J. Alexander. 1998. A protective role for IL-6 during early infection with *Toxoplasma gondii*. *Parasite Immunol.* 20: 231–239.
55. Allie, N., S. I. Grivennikov, R. Keeton, N.-J. Hsu, M.-L. Bourigault, N. Court, C. Fremond, V. Yeremeev, Y. Shebzukhov, B. Ryffel, et al. 2013. Prominent role for T cell-derived tumour necrosis factor for sustained control of *Mycobacterium tuberculosis* infection. *Sci. Rep.* 3: 1809.
56. Virna, S., M. Deckert, S. Lütjen, S. Soltek, K. E. Foulds, H. Shen, H. Körner, J. D. Sedgwick, and D. Schlüter. 2006. TNF is important for pathogen control and limits brain damage in murine cerebral listeriosis. *J. Immunol.* 177: 3972–3982.
57. Fujita, M., S. Ikegame, E. Harada, H. Ouchi, I. Inoshima, K. Watanabe, S. Yoshida, and Y. Nakanishi. 2008. TNF receptor 1 and 2 contribute in different ways to resistance to *Legionella pneumophila*-induced mortality in mice. *Cytokine* 44: 298–303.
58. Ferrero, M. C., M. S. Hielpos, N. B. Carvalho, P. Barrionuevo, P. P. Corsetti, G. H. Giambartolomei, S. C. Oliveira, and P. C. Baldi. 2014. Key role of Toll-like receptor 2 in the inflammatory response and major histocompatibility complex class ii downregulation in *Brucella abortus*-infected alveolar macrophages. *Infect. Immun.* 82: 626–639.
59. Pietras, E. M., L. S. Miller, C. T. Johnson, R. M. O'Connell, P. W. Dempsey, and G. Cheng. 2011. A MyD88-dependent IFNγR-CCR2 signaling circuit is required for mobilization of monocytes and host defense against systemic bacterial challenge. *Cell Res.* 21: 1068–1079.
60. De Trez, C., S. Magez, S. Akira, B. Ryffel, Y. Carlier, and E. Muraille. 2009. iNOS-producing inflammatory dendritic cells constitute the major infected cell type during the chronic *Leishmania major* infection phase of C57BL/6 resistant mice. *PLoS Pathog.* 5: e1000494.
61. Iwakura, Y., H. Ishigame, S. Saijo, and S. Nakae. 2011. Functional specialization of interleukin-17 family members. *Immunity* 34: 149–162.
62. Curtis, M. M., and S. S. Way. 2009. Interleukin-17 in host defence against bacterial, mycobacterial and fungal pathogens. *Immunology* 126: 177–185.
63. Tsai, H. C., S. Velichko, L. Y. Hung, and R. Wu. 2013. IL-17A and Th17 cells in lung inflammation: an update on the role of Th17 cell differentiation and IL-17R signaling in host defense against infection. *Clin. Dev. Immunol.* 2013: 267971.
64. Duhen, R., S. Glatigny, C. A. Arbelaez, T. C. Blair, M. Oukka, and E. Bettelli. 2013. Cutting edge: the pathogenicity of IFN-γ-producing Th17 cells is independent of T-bet. *J. Immunol.* 190: 4478–4482.
65. Skyberg, J. A., T. Thornburg, M. Rollins, E. Huarte, M. A. Jutila, and D. W. Pascual. 2011. Murine and bovine γδ T cells enhance innate immunity against *Brucella abortus* infections. *PLoS One* 6: e21978.
66. Wozniak, K. L., J. K. Kolls, and F. L. Wormley, Jr. 2012. Depletion of neutrophils in a protective model of pulmonary cryptococcosis results in increased IL-17A production by γδ T cells. *BMC Immunol.* 13: 65.
67. Dejima, T., K. Shibata, H. Yamada, H. Hara, Y. Iwakura, S. Naito, and Y. Yoshikai. 2011. Protective role of naturally occurring interleukin-17A-producing γδ T cells in the lung at the early stage of systemic candidiasis in mice. *Infect. Immun.* 79: 4503–4510.
68. Cheng, P., T. Liu, W.-Y. Zhou, Y. Zhuang, L. S. Peng, J. Y. Zhang, Z. N. Yin, X. H. Mao, G. Guo, Y. Shi, and Q. M. Zou. 2012. Role of gamma-delta T cells in host response against *Staphylococcus aureus*–induced pneumonia. *BMC Immunol.* 13: 38.
69. Skyberg, J. A., T. Thornburg, I. Kochetkova, W. Layton, G. Callis, M. F. Rollins, C. Riccardi, T. Becker, S. Golden, and D. W. Pascual. 2012. IFN-γ-deficient mice develop IL-1-dependent cutaneous and musculoskeletal inflammation during experimental brucellosis. *J. Leukoc. Biol.* 92: 375–387.
70. MacNamara, K. C., K. Oduro, O. Martin, D. D. Jones, M. McLaughlin, K. Choi, D. L. Borjesson, and G. M. Winslow. 2011. Infection-induced myelopoiesis during intracellular bacterial infection is critically dependent upon IFN-γ signaling. *J. Immunol.* 186: 1032–1043.
71. Barquero-Calvo, E., A. Martirosyan, D. Ordoñez-Rueda, V. Arce-Gorvel, A. Alfaro-Alarcón, H. Lepidi, B. Malissen, M. Malissen, J. P. Gorvel, and E. Moreno. 2013. Neutrophils exert a suppressive effect on Th1 responses to intracellular pathogen *Brucella abortus*. *PLoS Pathog.* 9: e1003167.
72. Cheng, O. Z., and N. Palaniyar. 2013. NET balancing: a problem in inflammatory lung diseases. *Front. Immunol.* 4: 1.
73. Durward, M., G. Radhakrishnan, J. Harms, C. Bareiss, D. Magnani, and G. A. Splitter. 2012. Active evasion of CTL mediated killing and low quality responding CD8+ T cells contribute to persistence of brucellosis. *PLoS One* 7: e34925.
74. Durward-Diioia, M., J. Harms, M. Khan, C. Hall, J. A. Smith, and G. A. Splitter. 2015. CD8+ T cell exhaustion, suppressed gamma interferon production, and delayed memory response induced by chronic *Brucella melitensis* infection. *Infect. Immun.* 83: 4759–4771.
75. Clapp, B., J. A. Skyberg, X. Yang, T. Thornburg, N. Walters, and D. W. Pascual. 2011. Protective live oral brucellosis vaccines stimulate Th1 and th17 cell responses. *Infect. Immun.* 79: 4165–4174.